

WCAP-10457

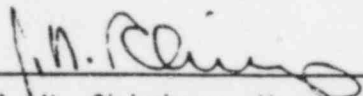
WESTINGHOUSE PROPRIETARY CLASS 3

THE EFFECTS OF THERMAL AGING ON THE  
STRUCTURAL INTEGRITY OF CAST STAINLESS STEEL  
PIPING FOR WESTINGHOUSE NUCLEAR  
STEAM SUPPLY SYSTEMS

November, 1983

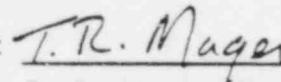
W. H. Bamford  
M. K. Kunka  
J. Spitznagel  
F. J. Witt

APPROVED:



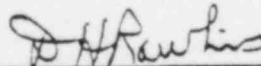
J. N. Chirigos, Manager  
Structural Materials Engineering

APPROVED:



T. R. Mager, Manager  
Metallurgical and NDE Analysis

APPROVED:



D. H. Rawlins  
Product Licensing

8312250258 831219  
PDR TOPRP EMVWEST  
B PDR

WESTINGHOUSE ELECTRIC CORPORATION

Nuclear Energy Systems  
P.O. Box 355  
Pittsburgh, Pennsylvania 15230

## WESTINGHOUSE PROPRIETARY CLASS 3

## TABLE OF CONTENTS

SECTION	TITLE	PAGE
1	INTRODUCTION	1-1
2	EFFECT OF THERMAL AGING ON THE FRACTURE TOUGHNESS PROPERTIES OF CAST STAINLESS STEEL	2-1
	2.1 Introduction	2-1
	2.2 Paper by Landerman and Bamford (Reference 2)	2-1
	2.2.1 The Test Program	2-1
	2.2.2 Material	2-2
	2.2.3 Mechanical Properties	2-2
	2.2.4 Tensile Tests	2-3
	2.2.5 Charpy V-Impact Tests	2-3
	2.2.6 J-Integral Tests	2-3
	2.2.7 Fatigue Crack Growth Data	2-5
	2.2.8 Conclusion	2-6
	2.3 Paper by Bamford, Landerman and Diaz (Reference 3)	2-6
	2.4 Paper by Slama, Petrequin, Masson and Mager (Reference 4)	2-7
	2.5 Confirmatory Westinghouse Results	2-9
	2.6 Conclusions	2-10
3	MECHANISMS OF THERMAL AGING	3-1
4	FRACTURE ASSESSMENT IN AUSTENITIC STAINLESS STEEL PIPING	4-1
	4.1 Methodology	4-1
	4.2 Experimental Verification	4-2
	4.3 Bending Tests and Aged Piping	4-4
	4.4 Stability Analysis Based on Tearing Modulus	4-7
5	EFFECTS OF THERMAL AGING ON WESTINGHOUSE SUPPLIED CENTRIFUGALLY CAST REACTOR COOLANT PIPING	5-1
	5.1 Production and Quality Assurance	5-1
	5.2 End-of-Life Toughness Predictions	5-2
	5.3 Plant Specific End-of-Life Reactor Coolant Piping Toughness	5-4
6	SUMMARY AND CONCLUSIONS	6-1
7	REFERENCES	7-1
APPENDIX A	DETERMINATION OF THE MOMENT CAPACITY OF PRESSURIZED PIPING WITH CIRCUMFERENTIALLY-ORIENTED FLAWS	A-1

## WESTINGHOUSE PROPRIETARY CLASS 3

## LIST OF TABLES

TABLE	TITLE	PAGE
2.2-1	CHEMICAL ANALYSIS OF STEELS TESTED (WEIGHT PERCENT)	2-13
2.2-2	HEAT TREATMENT AND TENSILE PROPERTIES OF A351 CF8M AT 650°F (343°C)	2-14
2.2-3	EFFECT OF AGING AT 800°F (427°C) ON TENSILE PROPERTIES OF TYPE 316 A351 CF8M CENTRIFUGALLY CAST STAINLESS STEEL HEAT C1488	2-15
2.2-4	CHARPY IMPACT TEST RESULTS - EFFECT OF AGING TIME AT 800°F (427°C) - ROOM TEMPERATURE TESTS CENTRIFUGALLY CAST A351 CF8M	2-16
2.2-5	SUMMARY OF RESULTS - TOUGHNESS OF CF8M STAINLESS PIPING MATERIAL	2-17
2.3-1	CHEMISTRY OF CAST PIPE USED IN BURST TESTS OF AGED PIPE	2-18
2.3-2	AGED PIPE TENSILE PROPERTIES	2-18
2.5-1	TENSILE PROPERTIES	2-19
2.6-1	SUMMARY OF AVERAGE TOUGHNESS PROPERTIES 316 CF8M	2-20
3.1	THIN FILM ANALYSIS	3-6
5.1	CHEMICAL AND PHYSICAL PROPERTIES OF PLANT A REACTOR COOLANT PIPING	5-5
5.2	CHEMICAL AND PHYSICAL PROPERTIES OF PLANT B REACTOR COOLANT PIPING	5-6
5.3	CHEMICAL AND PHYSICAL PROPERTIES OF PLANT C REACTOR COOLANT PIPING	5-7
5.4	CHEMICAL AND PHYSICAL PROPERTIES OF PLANT D REACTOR COOLANT PIPING	5-8
5.5	CHEMICAL AND PHYSICAL PROPERTIES OF PLANT E REACTOR COOLANT PIPING	5-9
5.6	CHEMICAL AND PHYSICAL PROPERTIES OF PLANT F REACTOR COOLANT PIPING	5-10
5.7	CHEMICAL AND PHYSICAL PROPERTIES OF PLANT G REACTOR COOLANT PIPING	5-11
5.8	CHEMICAL AND PHYSICAL PROPERTIES OF PLANT H REACTOR COOLANT PIPING	5-12

## LIST OF TABLES (cont'd)

TABLE	TITLE	PAGE
5.9	CHEMICAL AND PHYSICAL PROPERTIES OF PLANT I REACTOR COOLANT PIPING	5-13
5.10	CHEMICAL AND PHYSICAL PROPERTIES OF PLANT J REACTOR COOLANT PIPING	5-14

## LIST OF FIGURES

FIGURE	TITLE	PAGE
2.2-1	SPECIMEN ORIENTATIONS IN PIPING MATERIAL	2-21
2.2-2	EFFECT OF AGING TIME ON TENSILE PROPERTIES - CONVERSION FACTOR $\text{KSI} \times 6.894757 \times 10^6 = \text{Pa}$	2-22
2.2-3	EFFECT OF AGING TIME ON CHARPY IMPACT RESULTS - CONVERSION FACTORS: $\text{FT-LB} \times 1.355818 = \text{JOULES}$ ; $\text{MILS} \times 2.54 \times 10^{-5} = \text{METERS}$	2-23
2.2-4	AGING EFFECTS ON $J_{IC}$ AT ROOM TEMPERATURE 316 CAST STAINLESS STEEL-CONVERSION FACTORS: $\text{IN} \times 2.54 \times 10^{-2} = \text{m}$ , $\text{IN-LB/IN}^2 \times 0.0001751 = \text{MJ/m}$	2-24
2.2-5	AGING EFFECTS ON $J_{IC}$ AT 600°F (343°C) - 316 STAINLESS STEEL - CONVERSION FACTORS: $\text{IN} \times 2.54 \times 10^{-2} = \text{m}$ , $\text{IN-LB/IN}^2 \times 0.0001751 = \text{MJ/m}$	2-25
2.2-6	COMPARISON OF FATIGUE CRACK GROWTH RESULTS FOR AGED AND UNAGED 316 CAST STAINLESS STEEL IN PWR ENVIRONMENT	2-26
2.2-7	USE OF WALKER MODEL TO CORRELATE FATIGUE CRACK GROWTH RESULTS AGED AND UNAGED 316 CAST STAINLESS STEEL IN PWR ENVIRONMENT	2-27
2.3-1	SPECIMEN ORIENTATIONS IN FOUR INCH PIPE MATERIAL (SCHEMATIC)	2-28
2.3-2	CHARPY V-NOTCH ENERGY CURVE FOR VARIOUS AGING TIMES FOUR INCH PIPE MATERIAL	2-29
2.3-3	J-R CURVE FOR FOUR INCH PIPE MATERIAL	2-30
2.4-1	INFLUENCE OF AGING ON TENSILE PROPERTIES OF A WELD	2-31
2.4-2	INFLUENCE OF AGING ON THE ELONGATION AND REDUCTION OF AREA OF A WELD	2-32
2.4-3	INFLUENCE OF AGING ON IMPACT CHARPY TOUGHNESS (KCU)	2-33
2.4-4	HEAT B YIELD STRENGTH AND RUPTURE STRENGTH AS A FUNCTION OF TIME AGING	2-34
2.4-5	HEAT B ELONGATION AND REDUCTION OF AREA AS A FUNCTION OF TIME OF AGING	2-35
2.4-6	HEAT B KCU IMPACT TOUGHNESS AS A FUNCTION OF TIME	2-36
2.4-7	HEAT B INFLUENCE OF TEST TEMPERATURE ON KCU IMPACT TOUGHNESS AFTER AGING 10,000 HOURS AT 400°C	2-37
2.4-8	J- $\Delta a$ CURVES FOR WELDS B AND D. ROOM TEMPERATURE (INTERRUPTED TESTS)	2-38

## LIST OF FIGURES (cont'd)

FIGURE	TITLE	PAGE
2.4-9	J- $\Delta a$ CURVES FOR VIRGIN AND AGED CAST STAINLESS STEEL	2-39
2.4-10	HEAT L J- $\Delta a$ CURVES AT DIFFERENT TEMPERATURES AGED MATERIAL (7500 HOURS AT 400°C)	2-40
2.4-11	HEAT L FATIGUE CRACK GROWTH RATE AT ROOM TEMPERATURE FOR VIRGIN AND AGED MATERIAL	2-41
2.4-12	HEAT L FATIGUE CRACK GROWTH RATE AT 320°C IN AIR AND IN PWR ENVIRONMENT (1 cpm)	2-42
2.5-1	CHARPY U-NOTCH ENERGY AT ROOM TEMPERATURE FOR HEAT L AS A FUNCTION OF AGING AT 750°F (400°C)	2-43
2.5-2	CHARPY V-NOTCH ENERGY AT ROOM TEMPERATURE AND 550°F FOR HEAT L AFTER THERMAL AGING AT 750°F FOR 7500 HOURS	2-44
2.5-3	J-INTERNAL RESULTS OF 200°F FROM HEAT L	2-45
2.5-4	J-INTEGRAL RESULTS OF 600°F FROM HEAT L	2-46
2.5-5	FIGURE 25 OF SLAMA'S MONTEREY PAPER: HEAT L - J- $\Delta a$ CURVES AT DIFFERENT TEMPERATURES. AGED MATERIAL (7500 HOURS AT 400°C)	2-47
3.1	LOW TEMPERATURE MISCIBILITY GAP IN Fe-Cr SYSTEM	3-7
3.2	SCHEMATIC OF THE SPINODAL MORPHOLOGY	3-8
3.3	CONCENTRATION PROFILES OF Fe-32 AT %Cr IN THE AS-QUENCHED CONDITION, AND AFTER AGING AT 470°F [16]	3-9
3.4	COARSENING OF PRECIPITATE STRUCTURE, AND T ARE AVERAGE CENTER-TO-CENTER SPACING AND THICKNESS OF PRECIPITATES, RESPECTIVELY. THE TIME EXPONENT OF THE COARSENING KINETICS IS APPROXIMATELY 0.1 [16]	3-10
3.5	ROOM-TEMPERATURE CHARPY V-NOTCH AS A FUNCTION OF ISOTHERMAL EXPOSURES OF WATER-QUENCHED Fe <sub>29</sub> Cr-4Mo-2Ni ALLOY [23]	3-11
3.6	HARDENING IN HIGH PURITY Fe-26 Cr-1 Mo Alloy on ISOTHERMAL EXPOSURE TO 650 TO 900°F (343 to 482°C)	3-12
3.7	INCREASE IN HARDNESS OF Fe-32 AT .% Cr DURING AGING AT 470°C [16]	3-13
4.1	FULLY PLASTIC STRESS DISTRIBUTION	4-10
4.2	COMPARISON OF [ ] PREDICTIONS WITH EXPERIMENTAL	4-11

## WESTINGHOUSE PROPRIETARY CLASS 3

## LIST OF FIGURES (cont'd)

FIGURE	TITLE	PAGE
4.3	COMPARISON OF FAILURE PREDICTIONS WITH EXPERIMENTAL RESULTS OF [24]	4-12
4.4	TEST ASSEMBLY OF FOUR INCH PIPING	4-13
4.5	PERTINENT DIMENSIONS OF AGED AND UNAGED PIPES AFTER TESTING	4-14
4.6	MOMENT-DEFLECTION CURVES FOR AGED AND UNAGED FOUR INCH SCHEDULE 80 PIPES	4-15
4.7	COMPARISON OF PREDICTED ACTUAL [ ] FOR TESTS OF AGED AND UNAGED PIPES	4-16
A.1	PIPE WITH A THROUGH-WALL FLAW	A-2

## SECTION 1

## INTRODUCTION

Cast stainless steel is one of the prime materials used for primary coolant piping. These cast materials can contain ferrite levels greater than 15 percent to produce improved yield and tensile properties. This steel has long been known to be susceptible to thermal aging at temperatures in excess of 800°F (427°C), and there is now evidence that thermal aging can occur at temperatures as low as [ ]<sup>†</sup> +a,c,e

Recent experimental work has been conducted to study the effects of long time thermal service on the properties of Type 316 cast stainless reactor coolant piping.<sup>[1,2]</sup> Results of these studies show that the flow properties of the steel are not strongly affected; the ultimate tensile strength is elevated slightly and the yield strength is essentially unchanged. The ductility is slightly reduced, as measured by the elongation and reduction in area from tensile tests. The Charpy impact energy and the  $J_{IC}$  properties of the steel are measurably degraded, however, and this information elicits the question of the effect of the aging process on the integrity of the piping.

In this report, experimental data obtained on several series of specimen tests are discussed, and two methodologies for assessing the integrity of piping components [ ]<sup>†</sup> are +a,c,e described. Justification is provided for the use of these methods for thermally aged piping through a series of burst tests conducted on actual aged material. A detailed discussion is also provided on the mechanism of damage induced by the aging process in the [ ]<sup>†</sup> temperature range, +a,c,e and a model for predicting the extent of damage as a function of time and temperature is reviewed and validated in terms of the mechanisms. This model is applied to the piping which exists in ten different plants, to predict their end-of-life properties as affected by the aging process. The results of application of the model are then discussed relative to available fracture properties, and the integrity of the piping is then evaluated for these plants.

## SECTION 2

EFFECT OF THERMAL AGING ON THE  
FRACTURE TOUGHNESS PROPERTIES OF CAST STAINLESS STEEL

## 2.1 INTRODUCTION

Thermal aging at elevated temperatures of cast stainless steels has been known for some time to reduce significantly the Charpy impact energy [1]. The implications of this behavior to fracture toughness parameters (K, J, T) have only been investigated in recent years [2,3,4]. In this section these recent works are reviewed and summarized. Recently obtained unpublished confirmatory fracture toughness results are also presented.

## 2.2 PAPER BY LANDERMAN AND BAMFORD (REFERENCE 2)

In this paper, results from test sections of cast Type 316 stainless steel (ASTM A351 CF8M) aged at 800°F for periods of 100 to 3000 hours are presented. These results are summarized below. Discussions of metallurgy and mechanisms in the paper are not summarized but are covered in detail in Section 3.

## 2.2.1 THE TEST PROGRAM

The test program consisted of evaluating changes in the Charpy impact values, tensile data, J-integral and fatigue crack growth rate data (both in air and pressurized water reactor [PWR] environments). The materials tested were in the following material conditions:

1. As received, solution annealed.
2. Condition (1) after aging at 800°F (427°C) for 100, 500, 1000, 2000, and 3000 hours, respectively.

Charpy V-notch (Cv) impact and tensile data were obtained in the unaged conditions and after aging at 800°F (427°C) for all aging times. The  $J_{IC}$  and fatigue crack growth tests were performed only in the unaged and 3000 hour aged condition.

### 2.2.2 MATERIAL

The materials used for the program were two heats of centrifugally cast stainless steel pipe, ASTM A351 Grade CF8M. The dimensions of the as-cast pipe were approximately 37 inches (.94 m) OD and 31 inches (.79 m) ID with a three-inch (.08 m) nominal wall. The chemical analyses and the as-received properties of the test materials are shown in Table 2.2-1 and Table 2.2-2.

Charpy V-notch specimens were taken in the axial (along the length of the pipe) and circumferential directions as shown in Figure 2.2-1. The length of the notch in the Charpy specimens was oriented perpendicular to the surface of the pipe. The Charpy V-notch specimens were taken with the axis of the specimen being at 1/4 thickness (T) location from the ID and OD of the pipe and at the center of the pipe, respectively. The tensile specimens were parallel to the length of the pipe at 1/4T and 3/4T locations (Figure 2.2-1). The compact tension specimens for the fatigue crack growth tests and the fracture toughness tests ( $J_{IC}$ ) were taken with the crack extension being perpendicular to the pipe thickness and the specimen notch being parallel to the length of the pipe, as shown in Figure 2.2-1.

### 2.2.3 MECHANICAL PROPERTIES

The aging process produced different effects on the range of mechanical properties measured. The tensile properties were essentially unaffected except for a moderate increase in the tensile strength and decrease in ductility; no significant effects were observed on fatigue crack growth behavior. The largest effect was observed on the Charpy impact properties, with a similar, but less severe effect on the measured  $J_{IC}$  values.

#### 2.2.4 TENSILE TESTS

The tensile results show slight hardening as evidenced by the increase in tensile strength and decreases in the total elongation and uniform elongation shown in Figure 2.2-2 and Table 2.2-3. It should be noted that the yield strength showed essentially no change.

#### 2.2.5 CHARPY V-IMPACT TESTS

The Charpy V-impact test results show a significant decrease from the unaged condition to the aged condition, 3000 hours at 800°F (427°C) (Figure 2.2-3 and Table 2.2-4). Although the absorbed energy for the specimens was slightly higher for the axial specimens compared to the circumferentially oriented specimens in the unaged condition, these differences were not noted after 1000 hours aging. The largest rate of properties change occurred during the first 100 hours of aging.

#### 2.2.6 J-INTEGRAL TESTS

Characterization of the fracture properties of the stainless steel was accomplished by determination of  $J_{IC}$  at both room temperature and 600°F (316°C) according to the present recommended practice of ASTM<sup>[5]</sup>. At the 600°F (316°C) temperature, tests were performed on both aged and unaged material of the same heat (C1488), while at room temperature only the aged material was tested. These results could be compared with results of an earlier series of tests on another heat of the same steel (C2375) in the unaged condition which were reported recently [6]. In all cases the tests employed "static" loading rates.

Results for both the aged and unaged material of both heats are summarized in Table 2.2-5. Only material aged for the maximum time of 3000 hours at 800°F (427°C) was tested. The  $J_{IC}$  values reported here for heat C2375 are somewhat different than those reported previously [6] because the recommended practice for J data interpretation has been revised and thus, the previous

data were reinterpreted to be consistent with the newly obtained properties. The value of  $J_{IC}$  for each combination of material and condition was determined by using the multiple specimen technique now recommended by ASTM<sup>[5]</sup>, where the subcritical crack extension was measured by heat tinting. The data are presented in Figures 2.2-4 and 2.2-5 for tests at room temperature and 600°F (316°C), respectively. The ASTM procedure precludes data points which are too close to the blunting line or those which display very large crack extensions. Several of the specimens tested fell into these categories, and so were not used in determining  $J_{IC}$ . These points are included for reference only in Figures 2.2-4 and 2.2-5. In all cases, except one, data for a single material and test temperature, have been used to obtain  $J_{IC}$ . In one case, however, data from two heats in the unaged condition were obtained at 600°F (316°C) and these data were combined in determining  $J_{IC}$  for this condition. The ellipses in Figure 2.2-5 encompass valid unaged data from the two heats, respectively, and emphasize the judgmental aspect of the R-curve drawn.

There was a clear effect of the aging process on the  $J_{IC}$  toughness values obtained at both room temperature and 600°F (316°C). The toughness measured at room temperature decreased from 2760 in-lb/in<sup>2</sup> (0.483 MJ/m<sup>2</sup>) to 2012 in. lb./in<sup>2</sup> (0.352 MJ/m<sup>2</sup>), while the toughness at 600°F (316°C) decreased somewhat more, from 2868 in. lb./in<sup>2</sup> (0.502 MJ/m<sup>2</sup>) to 1315 in. lb./in<sup>2</sup> (0.230 MJ/m<sup>2</sup>). As may be seen in Figures 2.2-4 and 2.2-5, the entire J-R curve changed with the aging process. Another measure of the fracture resistance of the material can be obtained from the slope of the J-resistance curve,  $dJ/da$  which describes the rate of increase in J above  $J_{IC}$ , as subcritical crack growth occurs. The room temperature tests showed that the aging process caused the slope to drop from a very steep value to a moderate slope. The slope of the J-resistance curve obtained at 600°F is judgmental as noted by the ellipses in Figure 2.2-5. Very little slope change due to aging is noted if the lines are examined. On the other hand the individual sets of data suggest a more substantial change with aging especially if only the data from heat 1488 are examined. A change in slope has been observed in more recent tests, to be discussed later.

## 2.2.7 FATIGUE CRACK GROWTH DATA

Fatigue crack growth rate tests were performed on a series of WOL type specimens 2 inches (5.08 cm) in thickness, in both air and pressurized water reactor (PWR) environments. In both environments the tests were conducted at 550°F (288°C), and the specimens were side-grooved for about five percent of the thickness. Tests were conducted only on material aged for 3000 hours at 800°F (427°C), and results were compared with data tests of the same heat (C2375) in PWR environment [7]. The results are summarized in Figures 2.2-6 and 2.2-7.

Results of the PWR fatigue crack growth rate tests are presented in Figure 2.2-6 and show that there is little, if any, effect on the crack growth rate results as a result of either the PWR environment or the aging process for crack growth rate tests at low R ratio. The data for the aged specimens scatters about the data obtained previously for the same heat in the unaged condition. Data were obtained on aged specimens under sinusoidal loadings at test frequencies ranging from one to twenty cycles per minute with no observable effect of frequency.

Somewhat unexpected results were obtained on the aged specimens tested at high R ratio, where the crack growth behavior showed large reversals near the beginning of the test, in each of the two specimens tested. One specimen, SW-34, showed unusually high growth rates before undergoing a large reversal which brought the rate down to the other data at the same R ratio. Because of the unusual behavior of the aged specimens, comparisons with the unaged results are difficult, but generally it may be seen in Figure 2.2-6 that aged and unaged material showed equivalent behavior. The effects of R ratio on the crack growth rates for this material can be successfully accounted for by use of the Walker model [8]. The Walker model involves a portrayal of fatigue crack growth rate data in terms of an "effective" stress intensity factor,  $K_{eff}$ , defined as

$$K_{eff} = K_{max} (1 - R)^X \quad (1)$$

where,  $K_{\max}$  = maximum applied stress intensity factor

$R$  = stress ratio ( $K_{\min}/K_{\max}$ )

$X$  = an empirical constant dependent on material and environment

The fatigue crack growth law then becomes:

$$\frac{da}{dN} = C K_{\text{eff}}^n \quad (2)$$

where,  $C$  and  $n$  are determined from test data.

The Walker model has the advantage of reducing to the conventional portrayal of crack growth as a function of  $\Delta K$  when the  $R$  ratio is zero. Results of interpreting the data in terms of the Walker model are presented in Figure 2.2-7.

### 2.2.8 CONCLUSION

The major conclusions reached in summarizing this paper are:

1. Although significant reductions in Charpy-V toughness were observed the changes in  $J_{IC}$  were not nearly as severe.
2. The crack growth characteristics of aged and unaged materials were comparable.

### 2.3 PAPER BY BAMFORD, LANDERMAN AND DIAZ (REFERENCE 3)

This paper is a follow-up of the one summarized in Section 2.2. Essentially a series of experiments were conducted to characterize the effects of high temperature service [ ] on the mechanical properties of cast stainless ferrite steel. The material studied was Type 316 CF8M stainless steel, which has a duplex structure consisting of ferrite and austenite. Tensile, Charpy and

J-integral R-curve properties were determined. To investigate the failure mode of thermally aged piping, entire sections of this heat of four inch (10.2 cm) schedule 80 cast piping were aged and tested to failure after the introduction of large flaws. The material was aged for 2000 hours at 800°F (427°C). The chemical composition of the material used in this investigation is given in Table 2.3-1. Orientation for the specimens tested is given in Figure 2.3-1.

The tensile properties obtained are presented in Table 2.3-2. As previously noted, an increase in ultimate strength was found with aging while the yield strength was almost unchanged. There was a slight decrease in total elongation with aging with a greater decrease noted for the reduction in area.

The change of Charpy V-notch energy with aging is shown in Figure 2.3-2. Interestingly, for temperatures of interest the major reduction in Charpy energy occurred in the first 500 hours of aging with no significant change noted thereafter.

The shelf energy was still near 100 ft-lbs (down from near 180 ft-lbs) after the 2000 hours of aging. An increase in transition temperature of close to 200°F is noted.

J-R curves for the material, aged and unaged, are given in Figure 2.3-3. No real effect of aging was discerned in these tests.

### 2.3.1 CONCLUSION

The major thrust of this paper is on the testing of piping, as discussed later. Perhaps the most significant observation from the material presented here is the rather dramatic increase in Charpy V-notch transition temperature as noted in Figure 2.3-2.

## 2.4 PAPER BY SLAMA, PETREQUIN, MASSON AND MAGER (REFERENCE 4)

Reference 4 is a most significant paper in that thermal aging effects on fracture toughness are examined for up to 10,000 hours, and a metallurgical model is set forth for evaluating such effects. The model is discussed in the next chapter.

Both welds and cast pipe were evaluated. The effects of aging on the tensile properties for the most highly sensitive of eight welds are given in Figures 2.4-1 and 2.4-2. Only a slight effect of aging is noted. In Figure 2.4-3 the Charpy U-notch impact energy is seen to decrease from around 7 daJ/cm<sup>2</sup> (40 ft-lbs) to near 4 daJ/cm<sup>2</sup> (24 ft-lbs). The welds are judged not to be overly sensitive to aging with the cast pipe being the limiting material.

Twelve heats of cast stainless steel were evaluated for thermal aging. Figures 2.4-4 and 2.4-5 summarize the effect of aging on the tensile properties for one of the most sensitive heats (Heat B). Slight increases of yield strength and elongation are noted while the ultimate strength is seen to increase significantly and the reduction of area decreases significantly. In Figure 2.4-6 the Charpy U-notch energy at room temperature is seen to decrease from 20 daJ/cm<sup>2</sup> (117 ft-lbs) to near 3 daJ/cm<sup>2</sup> (18 ft-lbs). In Figure 2.4-7, the energy is near 6 daJ/cm<sup>2</sup> (35 ft-lbs) at 300°C (570°F).

Room temperature fracture toughness properties of two unaged welds are given in Figure 2.4-8 compared with stainless steel plate. A  $J_{IC}$  of 130 to 150 kJ/m<sup>2</sup> (750 to 850 in-lb/in<sup>2</sup>) is noted. The tearing modulus is near 150 however.

Room temperature fracture toughness properties of unaged and aged heats (K and L) are given in Figure 2.4-9. The  $J_{IC}$  for aged Heat L is seen to be around 100 kJ/m<sup>2</sup> (571 in-lb/in<sup>2</sup>). The tearing modulus is between 50 and 55.

Higher temperature results for Heat L are given in Figure 2.4-10. Depending on test temperature and specimen,  $J_{IC}$  is seen to vary between 100 and 240 kJ/m<sup>2</sup> (571 and 1370 in-lb/in<sup>2</sup>). The tearing modulus at 320°C (600°F) can be estimated from the side-grooved specimen data to be between 40 and 65. The non-side grooved specimens yield a tearing modulus of 66.

Heat L was also used to investigate the effect of thermal aging on fatigue crack growth. These results are given in Figures 2.4-11 and 2.4-12. No significant effect of aging is noted, which is in agreement with the earlier work of Landerman and Bamford [2].

It should be noted that Heat L was found highly sensitive to thermal aging, having exhibited a Charpy U-notch energy of between 2.8 and 3.6 daJ/cm<sup>2</sup> (16-21 ft-lbs) at room temperatures after having been aged at 400°C (750°F) for 7500 hrs. Based on the model and discussion of Chapter 3, Heat L in the aged condition reported in [4] is judged to represent end-of-service-life properties for operating temperatures. [

]†

#### 2.4.1 CONCLUSION

The most significant points of the portion of the paper discussed here are as follows:

1. Even though the Charpy U-notch energy is significantly lowered by thermal aging of the most highly sensitive materials, the resistance to ductile crack extension remains reasonably high.
2. Thermal aging does not impact fatigue crack growth.

#### 2.5 CONFIRMATORY WESTINGHOUSE RESULTS

It has been postulated in the Slama et. al. paper [4] that Heat L which was thermally aged at 750°F for 7500 hours reached the end-of-life toughness in terms of Charpy U-notch impact energy (16-21) ft-lbs. at room temperature.

]†a,c,e



## 2.6 CONCLUSIONS

There are several significant observations and conclusions which may be made from the information presented in the previous sections. These are given below.

1. The literature cited is consistent in that the degradation of Charpy energy (V-notch and U-notch) at room temperature occurs early in the thermal aging process and proceeds at a decreasing rate thereafter.
2. The literature is consistent in that the yield strength is little effected by thermal aging (showing a slight increase) while the tensile strength may increase significantly; the reduction in area is significantly decreased.



## WESTINGHOUSE PROPRIETARY CLASS 3

TABLE 2.2-1 CHEMICAL ANALYSIS OF STEELS TESTED (WEIGHT PERCENT)

Element	Heat No.		
	C2375	C1488	
	Ladle	Ladle	Check
C	0.05	0.06	0.061
Mn	0.86	1.09	1.02
P	0.013	0.016	0.021
S	0.022	0.016	0.015
Si	0.74	0.75	0.63
Ni	9.46	10.45	9.48
Cr	19.93	20.80	20.95
Mo	2.55	2.62	2.63
N <sub>2</sub>	Not Reported	Not Reported	0.056
Co	0.06	0.077	Not Reported
Ferrite *	21	14	

\* Ferrite content based on Ladle analyses and using Schoefer Diagram  
 Nitrogen content in the check analysis for heat C1488 was included in the  
 calculation.

TABLE 2.2-2 HEAT TREATMENT AND TENSILE PROPERTIES OF A351 CF8M at 650°F (343°C)

Alloy	Condition	Temperature °C	0.2% Yield Strength		Tensile Strength		Elongation %	Reduction in Area %
			KSI	Mn/m <sup>2</sup>	KSI	Mn/m <sup>2</sup>		
Centrifugally cast type 316 A-351 CF8M Heat C2375	Annealed at 2050°F (1121°C) for 4 hours Water quenched	RT	46.0	317.4	75.4	520.3	41.0	55.5
		343	22.9	157.9	64.5	444.7		
Centrifugally cast type 316 A-351 CF8M Heat C1488	Annealed at 2050°F (1121°C) for 4 hours Water quenched	RT	38.3	264.3	83.2	574.1	40.5	70.7
		343	26.8	184.8	69.5	479.2	44.0	57.0

TABLE 2.2-3

EFFECT OF AGING AT 800°F (427°C) ON TENSILE PROPERTIES OF TYPE 316  
A351 CF8M CENTRIFUGALLY CAST STAINLESS STEEL HEAT C1488

Aging Time Hrs.	0.2% Yield Strength		Tensile Strength		Total Elongation %	Uniform Elongation %	RA %
	KSI	MN/m <sup>2</sup> Pa	KSI	MN/m <sup>2</sup> Pa			
0	25.8	177.9	68.7	473.7	45.0	37.5	59.7
0	26.2	180.6	67.1	462.6	42.9	35.5	66.9
100	26.2	180.6	73.9	509.5	35.9	30.2	59.1
100	28.0	193.1	73.1	504.0	34.0	30.2	55.2
500	25.6	176.5	78.9	544.0	33.5	29.4	51.3
500	26.9	185.5	78.5	541.9	34.8	29.9	48.3
1000	26.4	182.0	80.0	551.6	33.9	31.2	43.1
1000	26.5	182.7	79.4	547.4	34.9	31.4	41.1
2000	26.4	182.0	82.5	568.8	32.5	29.8	40.3
2000	27.1	185.8	80.4	554.3	32.1	29.0	44.9
3000	26.0	179.3	82.4	568.0	30.8	27.4	40.0
3000	27.9	192.4	82.2	566.7	30.5	28.7	37.7
Test Temperature-RT							
0	43.5	286.1	82.9	571.6	53.9	40.7	*
0	42.6	294.4	82.7	570.2	51.1	38.0	
100	42.2	290.9	91.7	632.2	46.3	34.3	
100	44.7	308.2	89.7	618.5	44.7	34.3	
500	42.4	292.3	96.5	665.3	43.6	32.7	
500	43.2	297.9	93.7	646.0	39.8	30.5	
1000	43.7	301.3	97.3	670.9	42.0	32.5	
1000	45.5	313.7	96.4	664.6	38.1	30.7	
2000	43.3	298.5	90.1	621.2	42.5	32.5	
2000	44.5	306.8	98.9	681.9	36.4	31.8	
3000	42.4	292.3	100.2	690.9	42.6	32.4	
3000	45.2	311.6	100.3	691.5	42.1	34.6	

\* Reduction in area not reported because all specimens deformed into an oval cross section.

TABLE 2.2-4  
 CHARPY IMPACT TEST RESULTS - EFFECT OF AGING  
 TIME AT 800°F (427°C) - ROOM TEMPERATURE TESTS  
 CENTRIFUGALLY CAST A351 CF8M

Aging Time Hrs.	<u>Axial Orientation</u>		<u>Circumferential Orientation</u>	
	Ft-lbs (Joules)	Lateral Expansion (mils)	Ft-lbs (Joules)	Lateral Expansion (mils)
0	177 (240)	105	147 (199)	99
0	145 (197)	105	161 (218)	110
0	183 (248)	107	133 (180)	112
100	129 (175)	97	110 (149)	87
100	151 (205)	90	119 (161)	92.5
100	103 (139)	87	100 (136)	89
500	61 (83)	49	59 (80)	58
500	47 (64)	44	45 (61)	46
500	45 (61)	49	46 (62)	47
1000	52 (71)	43	50 (68)	48
1000	53 (72)	45	40 (54)	39.5
1000	33 (45)	30	34 (45)	35
2000	40 (54)	39	40 (54)	42
2000	34 (46)	35	34 (46)	38
2000	29 (39)	24	26 (35)	27
3000	35 (47)	32	39 (53)	35
3000	29 (39)	31	32 (43)	34
3000	28 (38)	32	26 (35)	29

2-16

WESTINGHOUSE PROPRIETARY CLASS 3

TABLE 2.2-5 SUMMARY OF RESULTS - TOUGHNESS OF CF8M STAINLESS PIPING MATERIAL

<u>Material</u>	<u>Temperature (°C)</u>	<u><math>\sigma_f</math> (ksi)</u>	<u><math>J_{Ic}</math> (inlb/in<sup>2</sup>)</u>	<u><math>\frac{25 J_{Ic}}{\sigma_f}</math></u>	<u><math>\frac{dJ}{da}</math> (inlb/in<sup>3</sup>)</u>	<u>Number of Specimens</u>	<u>Range of <math>\Delta a</math> (inches)</u>
As received CF8M cast stainless Heat C237B	RT	60.7	2760	1.137	52061	9	0.090-0.288
Average of two heats							
As received CF8M cast stainless Heat C1488 Heat C237B	316	46.0	2868	1.559	16613 <sup>a</sup>	11	0.039-0.290
CF8M Cast Stainless Heat C1488 Aged 3000 hrs. @ 347°C	RT	62.5	2012	0.805	12109	6	0.021-0.179
	316	48.2	1315	0.682	15265	7	0.018-0.179

NOTE: (1) to convert inches to cm, multiply by 2.54  
 (2) to convert from inlb/in<sup>2</sup> to MJ/m<sup>2</sup> multiply by 0.0001751  
 (3) to convert from inlb/in<sup>3</sup> to MJ/m<sup>3</sup> multiply by 0.00689

<sup>a</sup>Using only the data from Heat C1488,  $\frac{dJ}{da}$  is near 60000 in-lb/in<sup>3</sup>

2-17

TABLE 2.3-1 CHEMISTRY OF CAST PIPE USED IN BURST TESTS OF AGED PIPE

GRADE	CASTING NUMBER	ANALYSIS (%)							FERRITE CONTENT
		C	Mn	Si	Ni	Cr	Mo	N	Schaeffler
SA 351 (CF8M)	8711	0.08	0.84	1.01	9.34	19.65	2.51		13.0

TABLE 2.3-2 AGED PIPE TENSILE PROPERTIES

Spec	Temperature (°F)	Yield Stress (ksi)	Ultimate Strength (ksi)	Total Elong. %	RA %
(A) WC-1	600	25.3	73.5	32.2	46.3
(A) WC-3	600	24.1	77.5	35.9	51.1
(A) WC-2	75	39.1	99.3	47.9	63.6
WC-4	600	25.1	67.9	38.6	58.3
WC-6	75	38.5	82.8	49.1	77.0

(A) Aged 2000 hrs. at 800F (427C)

TABLE 2.5-1: TENSILE PROPERTIES OF HEAT L

HEAT L: Solution annealed 1 hr. at 2050°F  
(1120°C) and water quenched on blank

TENSILE PROPERTIES ON HEAT L<sup>a</sup>

Test Temp. °F (°C)	Yield Strength	ksi (MPa)	Ultimate Strength	Reduction in Area (%)	Total Elongation
	<u>Unaged</u>				
RT	42.5 (293)	83.2 (573.5)	76.5	40	
650 (343)	26.0 (179)	65.8 (454)	49	25.6	
	(188)	68.0 (469)	63	30.2	
	<u>Aged 7500 hrs. at 750°F (400°C)</u>				
RT	45.4-47.9 (313-329)	108.3-109.2 (747-753)	30-26	49-35	
650 (343)	31.0-33.6 (214-232)	96.3-96.1 (664-663)	21-20	24-24	

<sup>a</sup> Creusot-Loire Data

TABLE 2.6-1 SUMMARY OF AVERAGE TOUGHNESS PROPERTIES  
HIGHLIGHTED IN THIS CHAPTER

316 CF8M

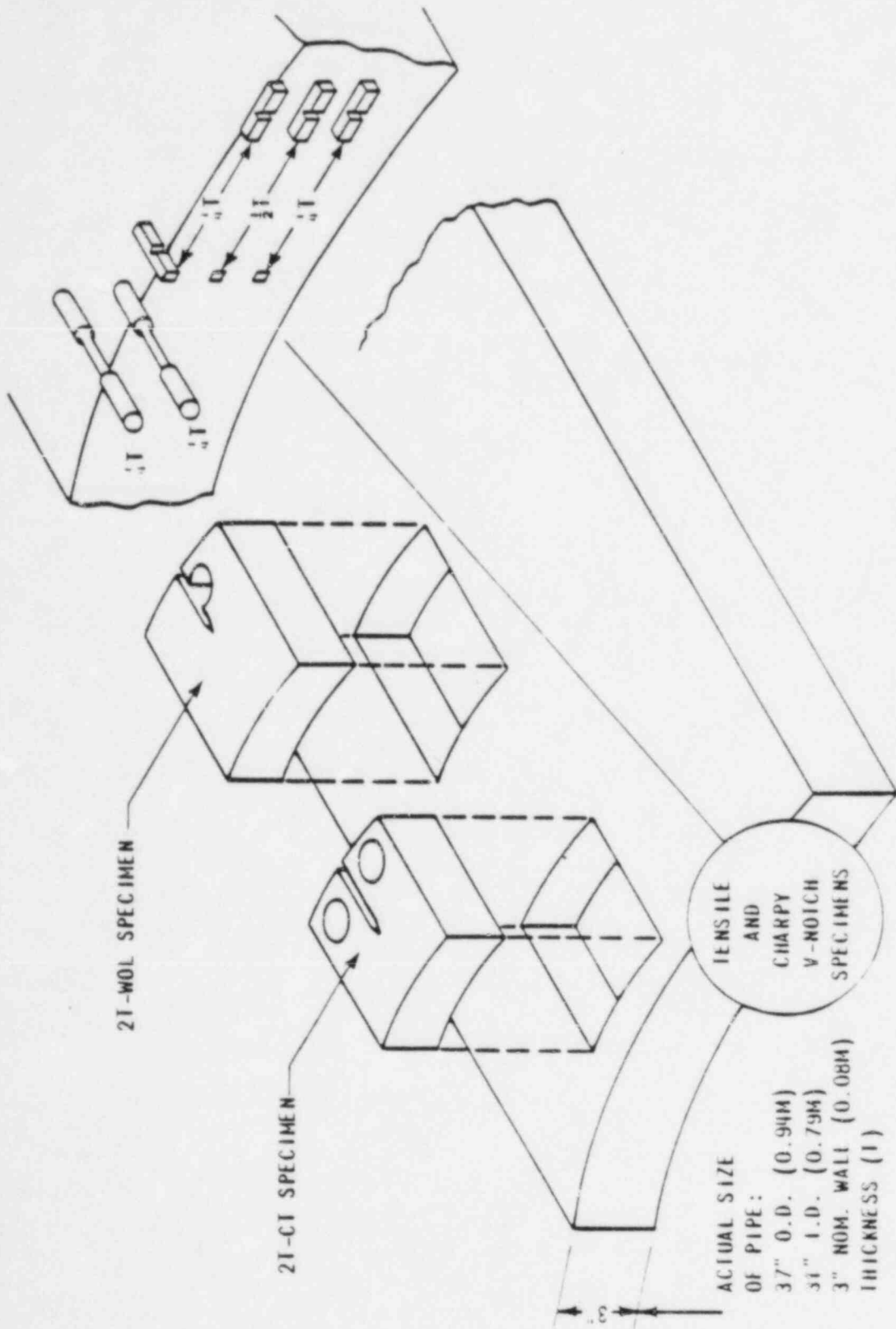


Figure 2.2-1 Specimen Orientations in Piping Material

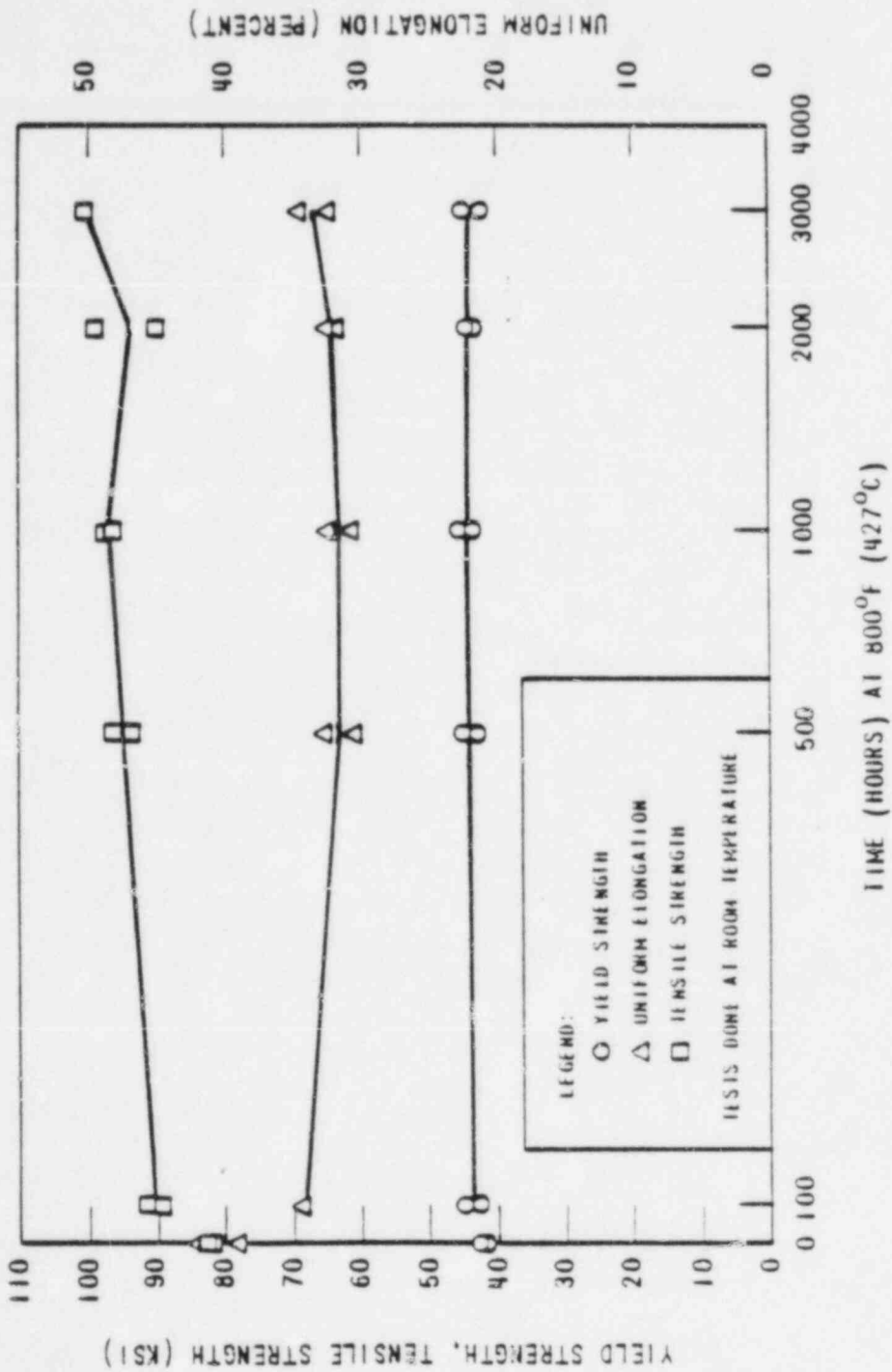


Figure 2.2-2 Effect of Aging Time on Tensile Properties - Conversion factor  
 KSI x 6.894757 x 10<sup>6</sup>-1.

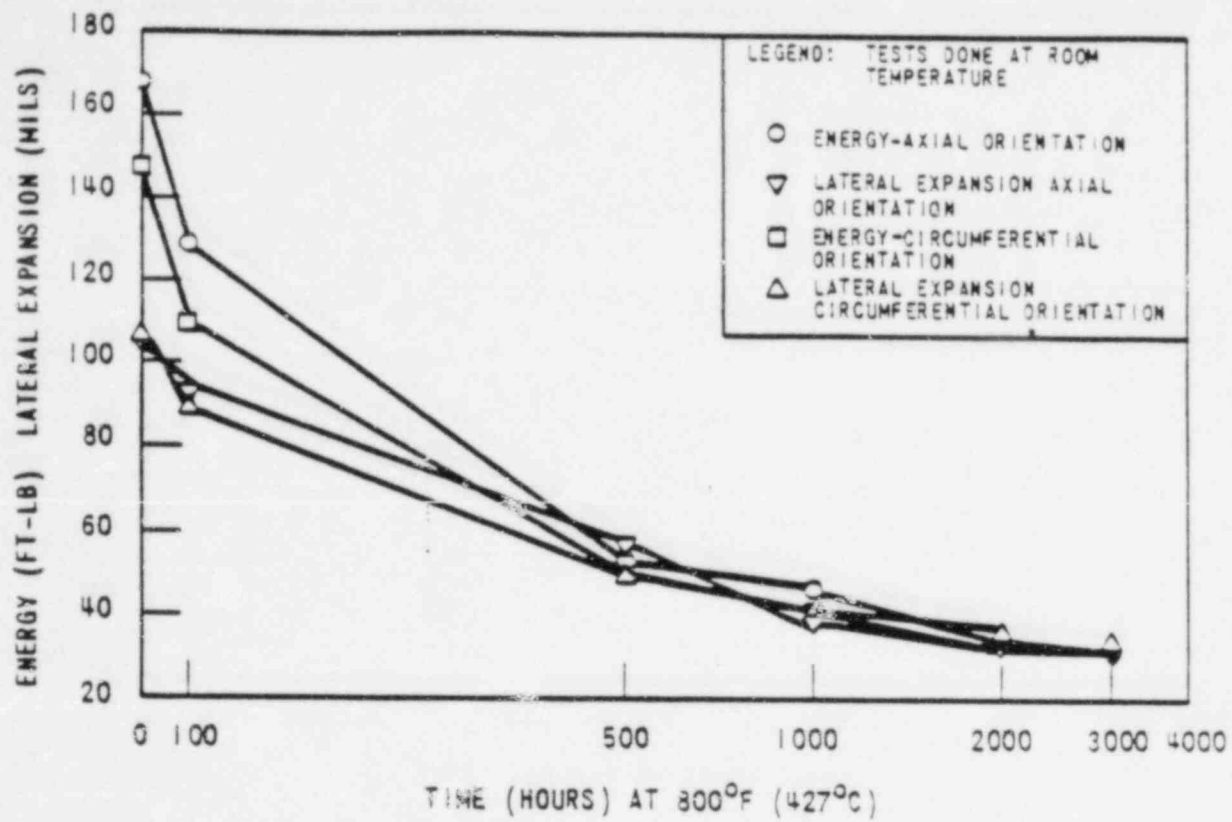


Figure 2.2-3 Effect of Aging Time on Charpy Impact Results - Conversion Factors: ft·lb x 1.355818 = Joules; Mil x  $2.54 \times 10^{-5}$  = Meters

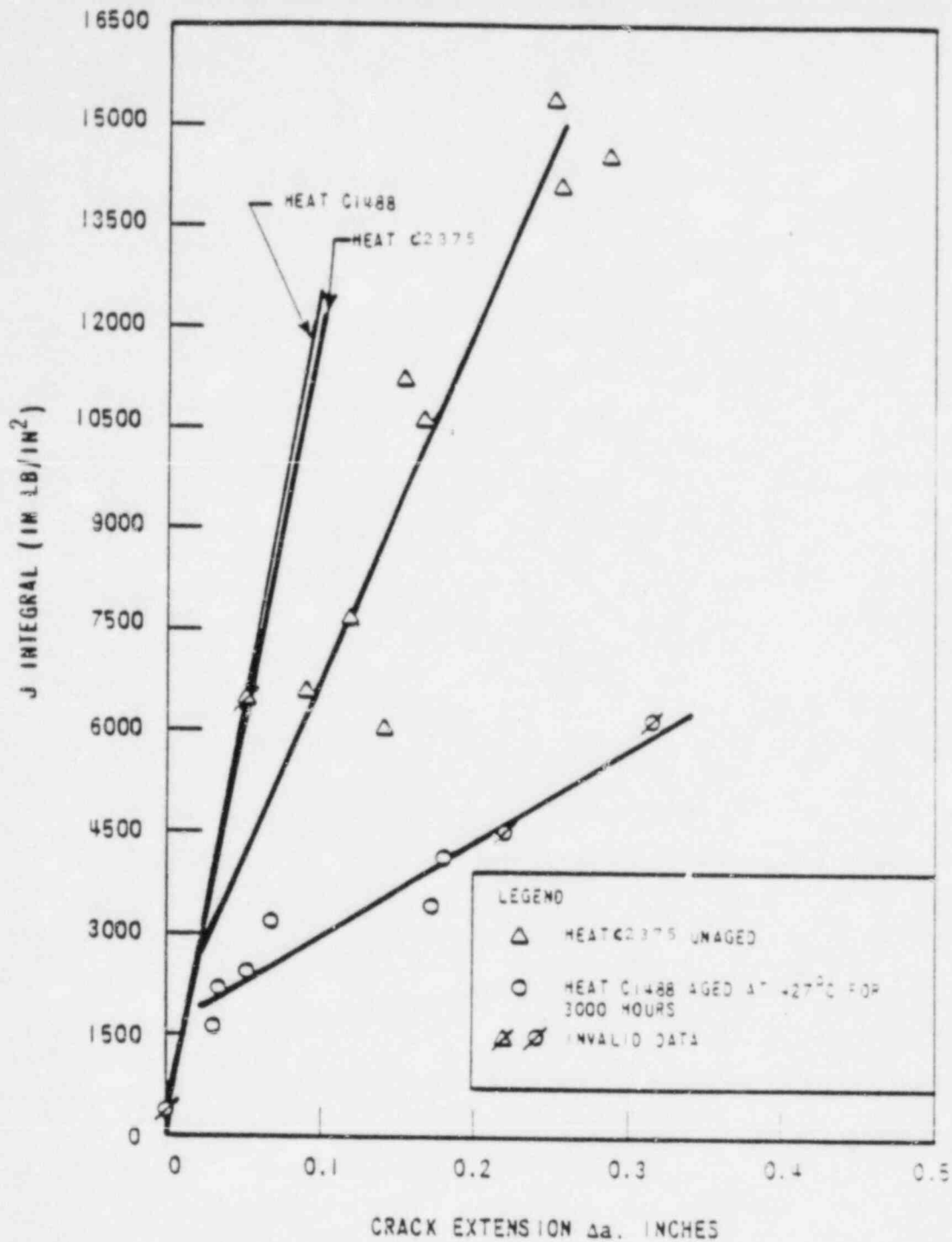


Figure 2.2-4 Aging Effects on  $J_{IC}$  at Room Temperature 316 Cast Stainless Steel Conversion Factors: in  $\times 2.54 \times 10^{-4}$  mm  
in-lb/in<sup>2</sup>  $\times 0.0001751$  = MJ/m

Figure 2.2-5 Aging Effects on  $J_{IC}$  at 600°F (343°C) - 316  
Stainless Steel - Conversion Factors: in x  
 $2.54 \times 10^{-2} = \text{m}$ , in-lb/in<sup>2</sup> x 0.0001751 = MJ/m

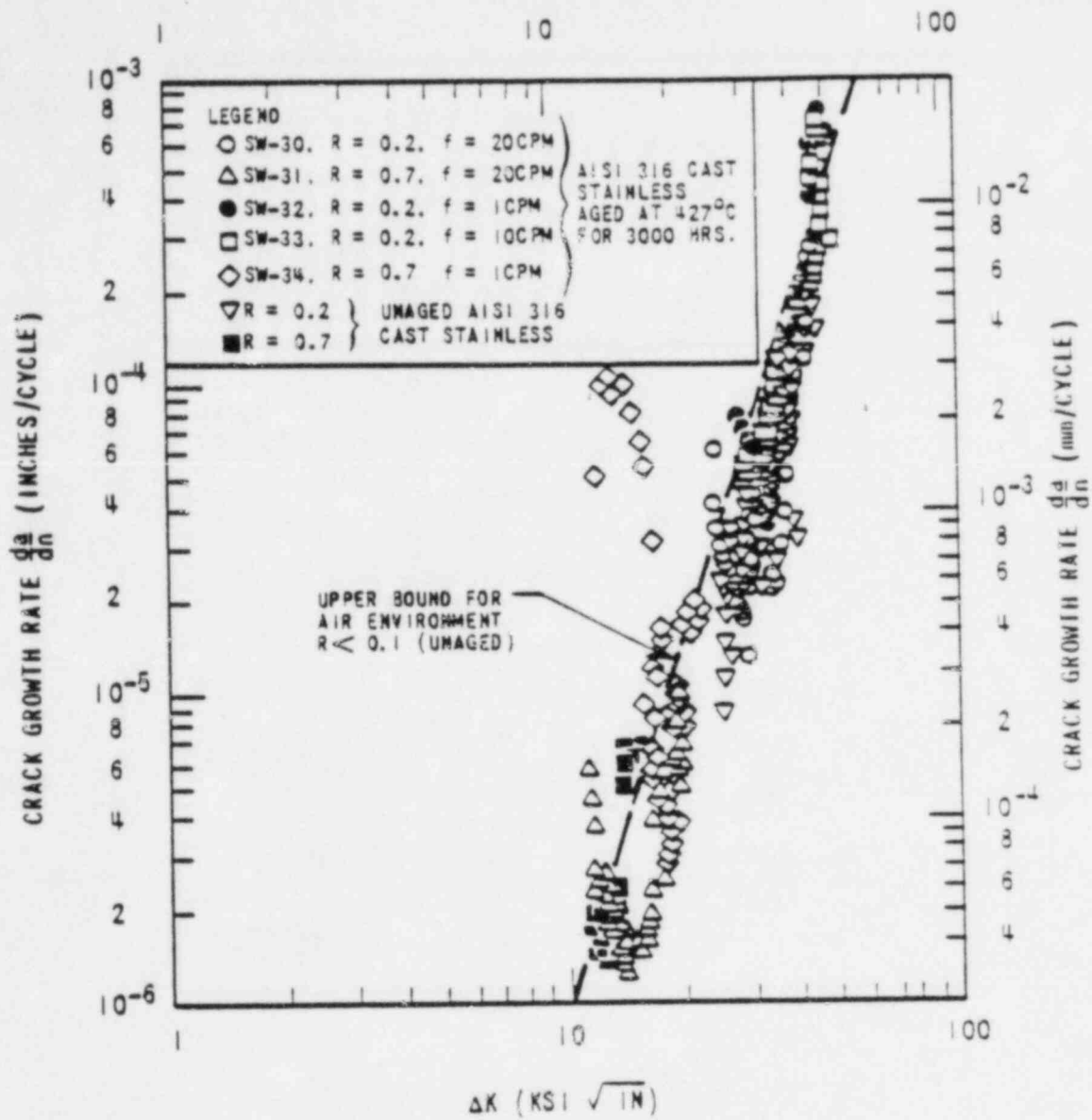


Figure 2.2-6 Comparison of Fatigue Crack Growth Results for Aged and Unaged 316 Cast Stainless Steel in PWR Environment

WESTINGHOUSE PROPRIETARY CLASS 3

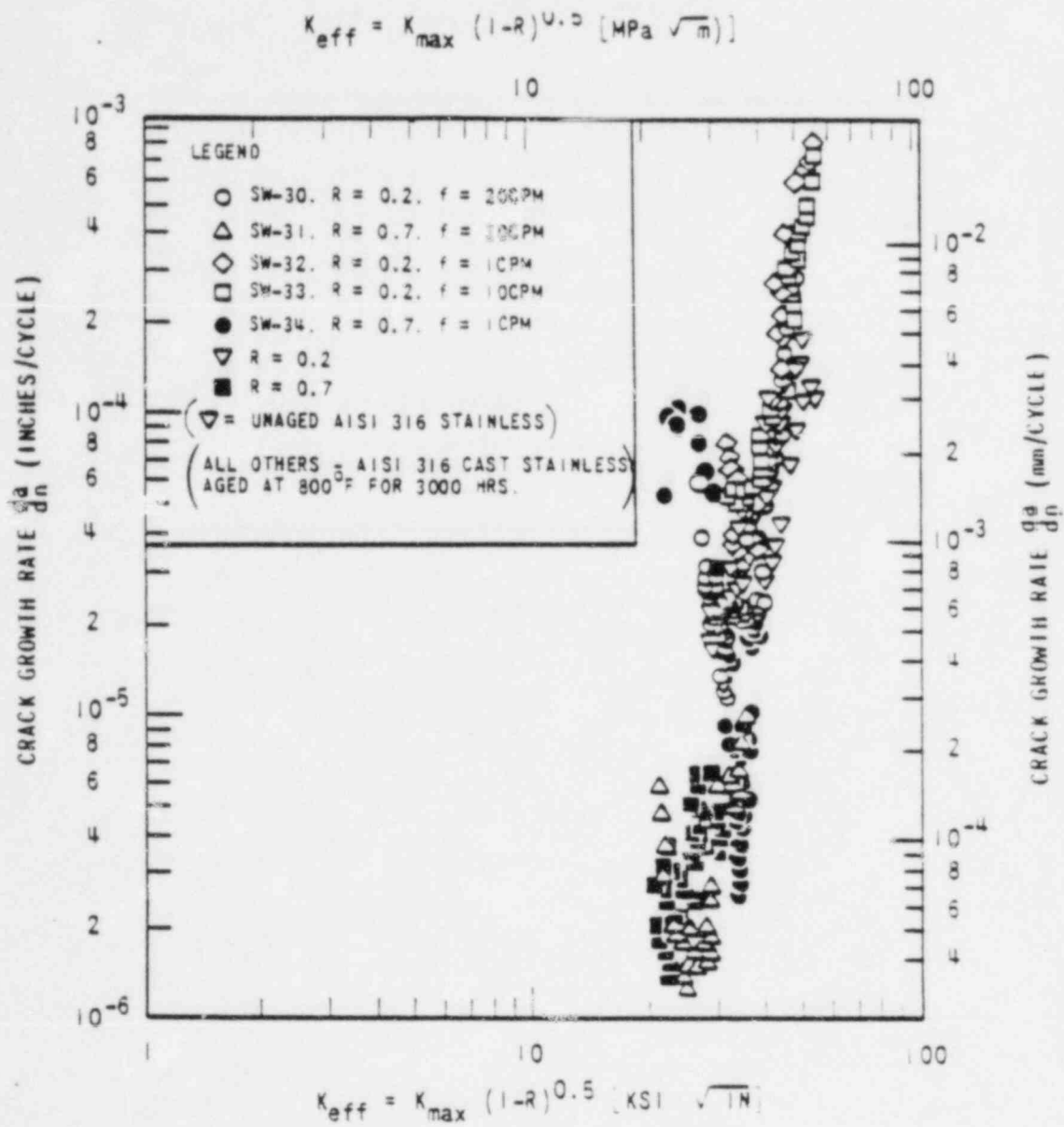


Figure 2.2-7 Use of Walker Model to Correlate Fatigue Crack Growth Results Aged and Unaged 316 Cast Stainless Steel in PWR Environment

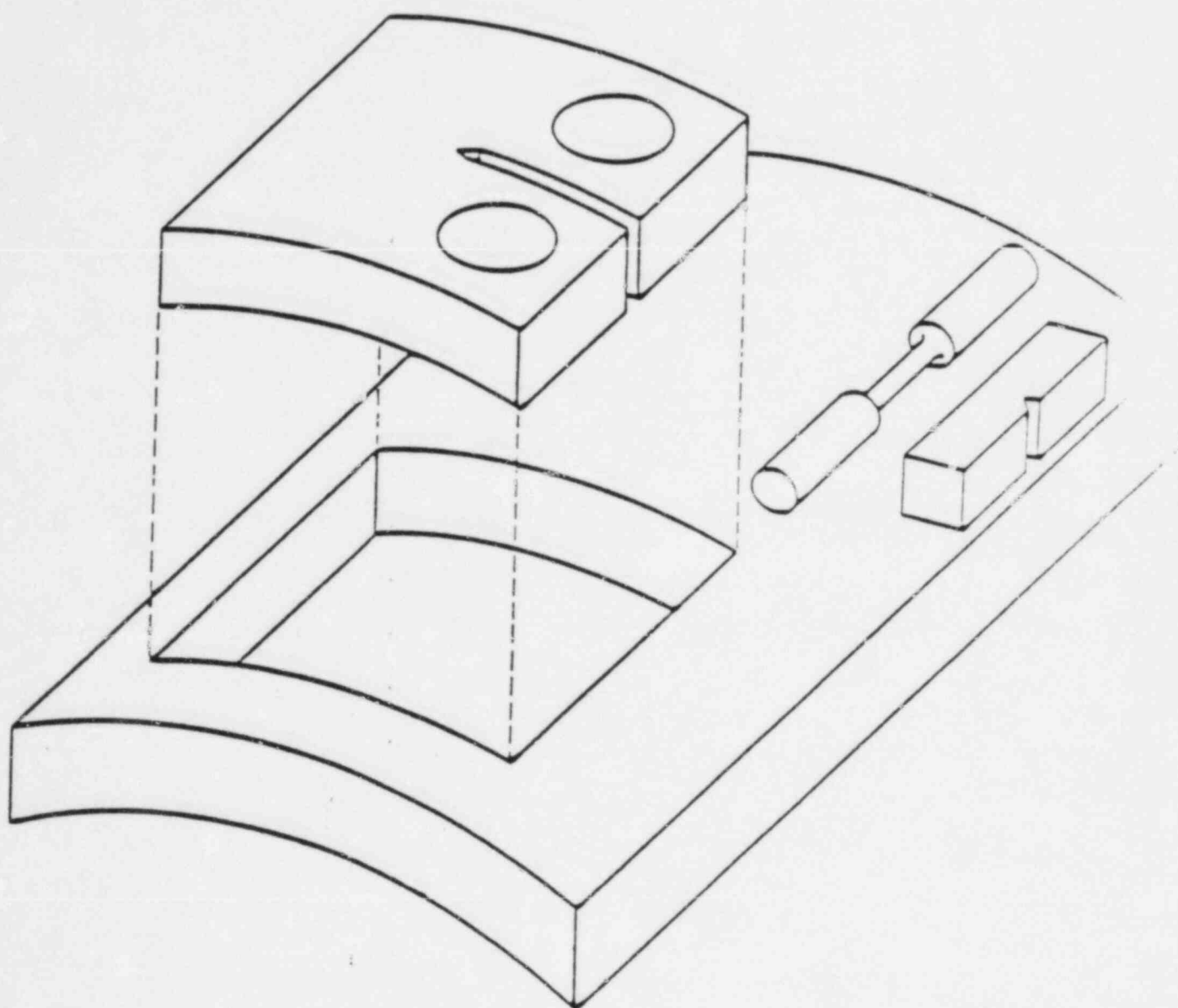


Figure 2.3-1 Specimen Orientations in Four Inch Pipe Material (Schematic)

## WESTINGHOUSE PROPRIETARY CLASS 3

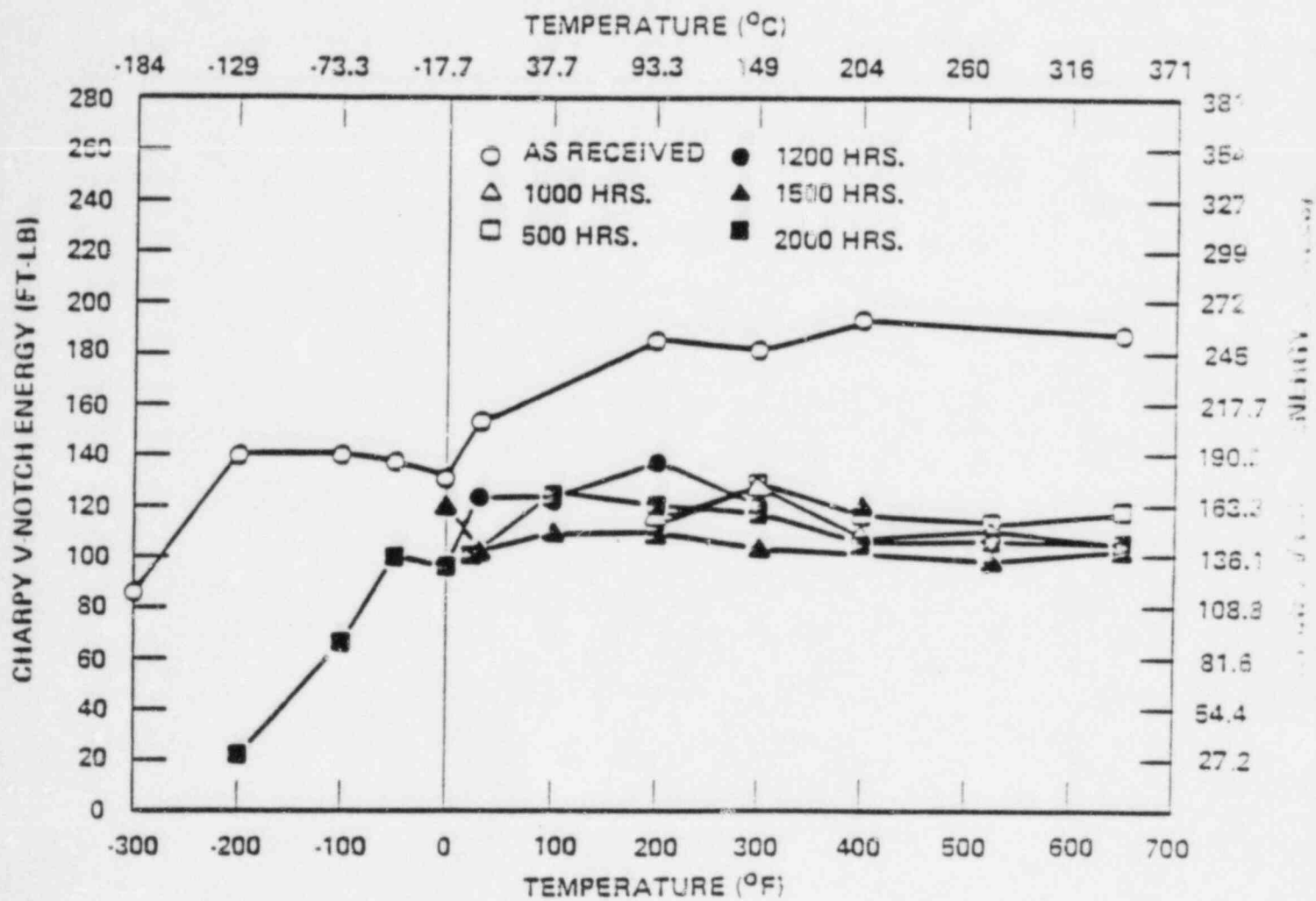


Figure 2.3-2 Charpy V-Notch Energy Curve for Various Aging Times  
Four Inch Pipe Material

J (IN. LB/IN.<sup>2</sup>)

Figure 2.3-3 J-R Curve for Four Inch Pipe Material

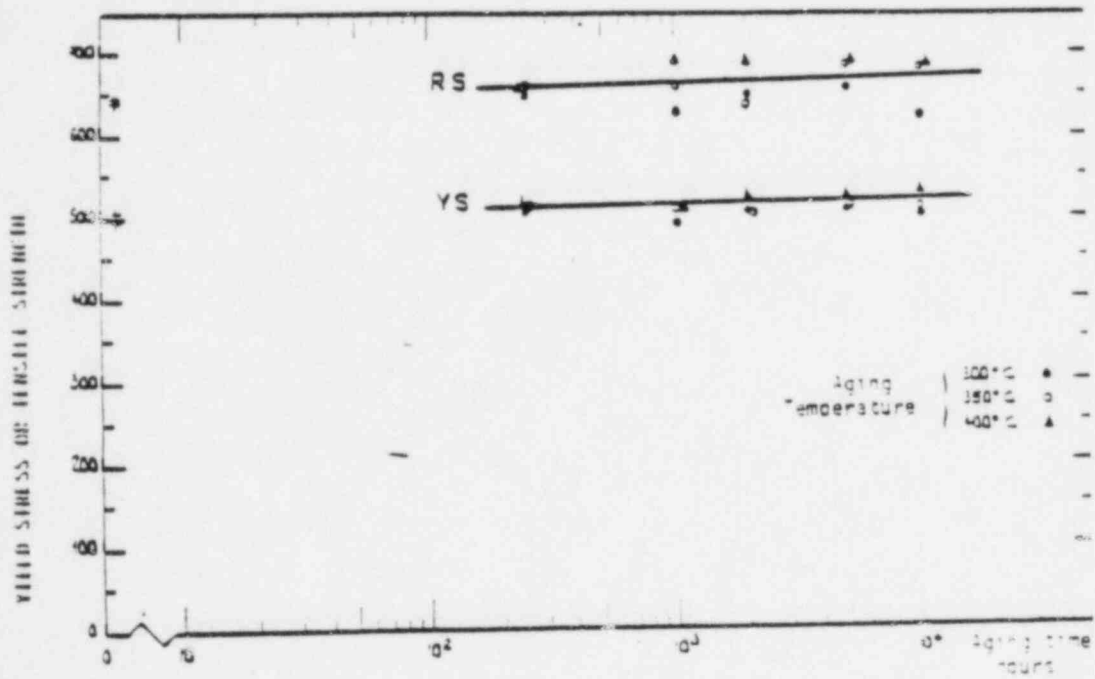


Figure 2.4-1: Influence of aging on tensile properties of a weld

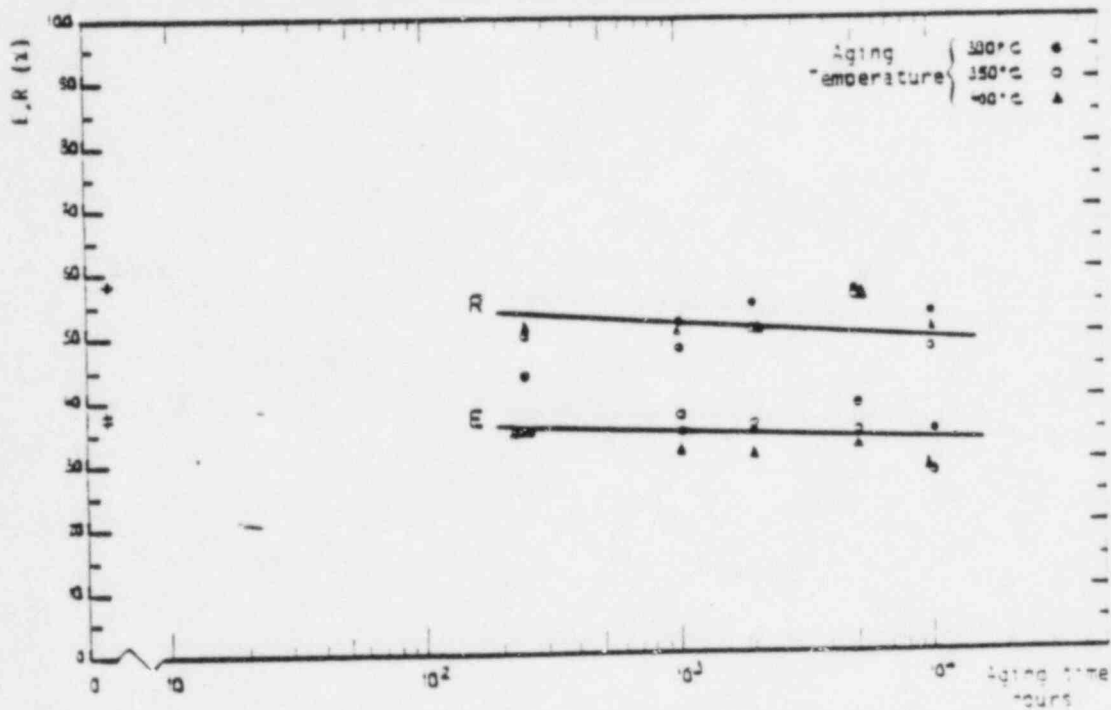


Figure 2.4-2: Influence of aging on the elongation and reduction of area of a weld

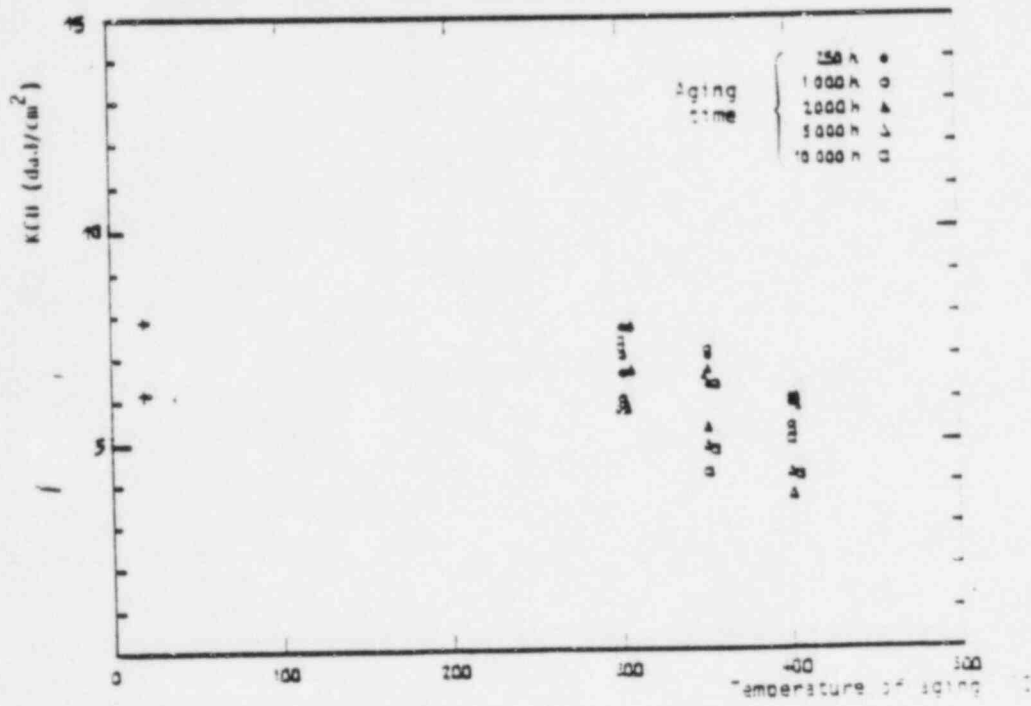


Figure 2.4-3 Influence of aging on impact Charpy toughness (KCU)

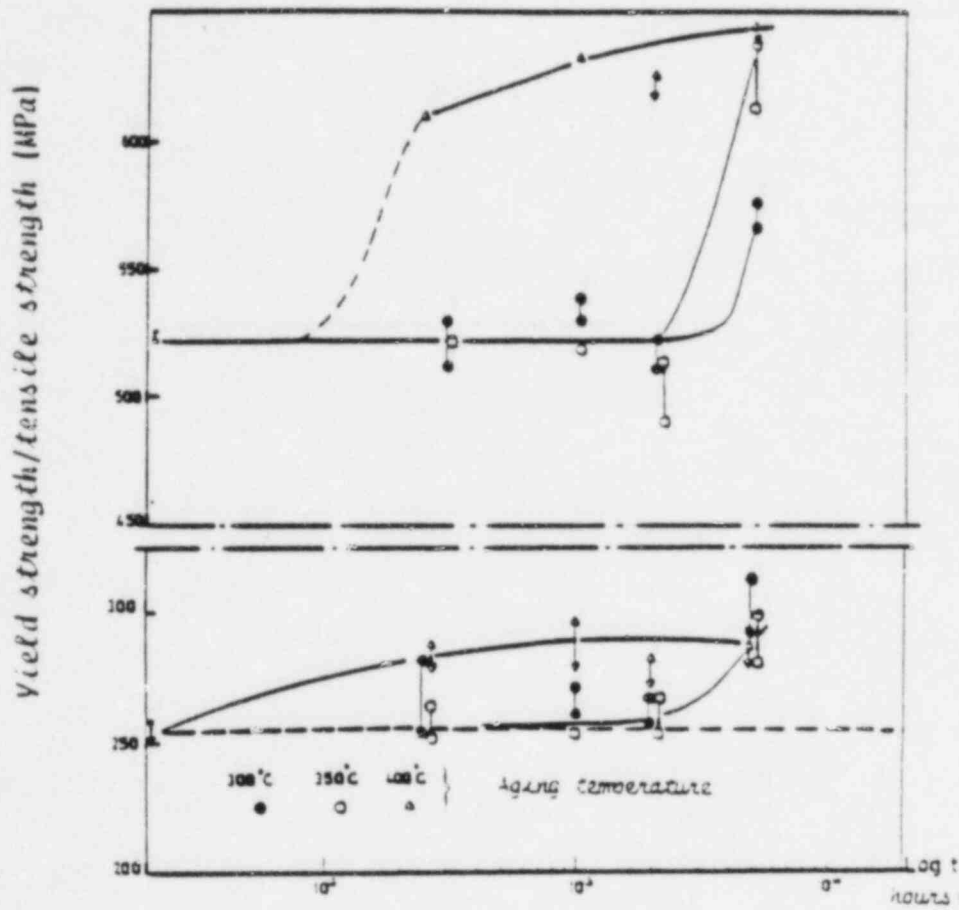


Figure 2.4-4: Heat B Yield Strength and rupture strength as a function of time aging.

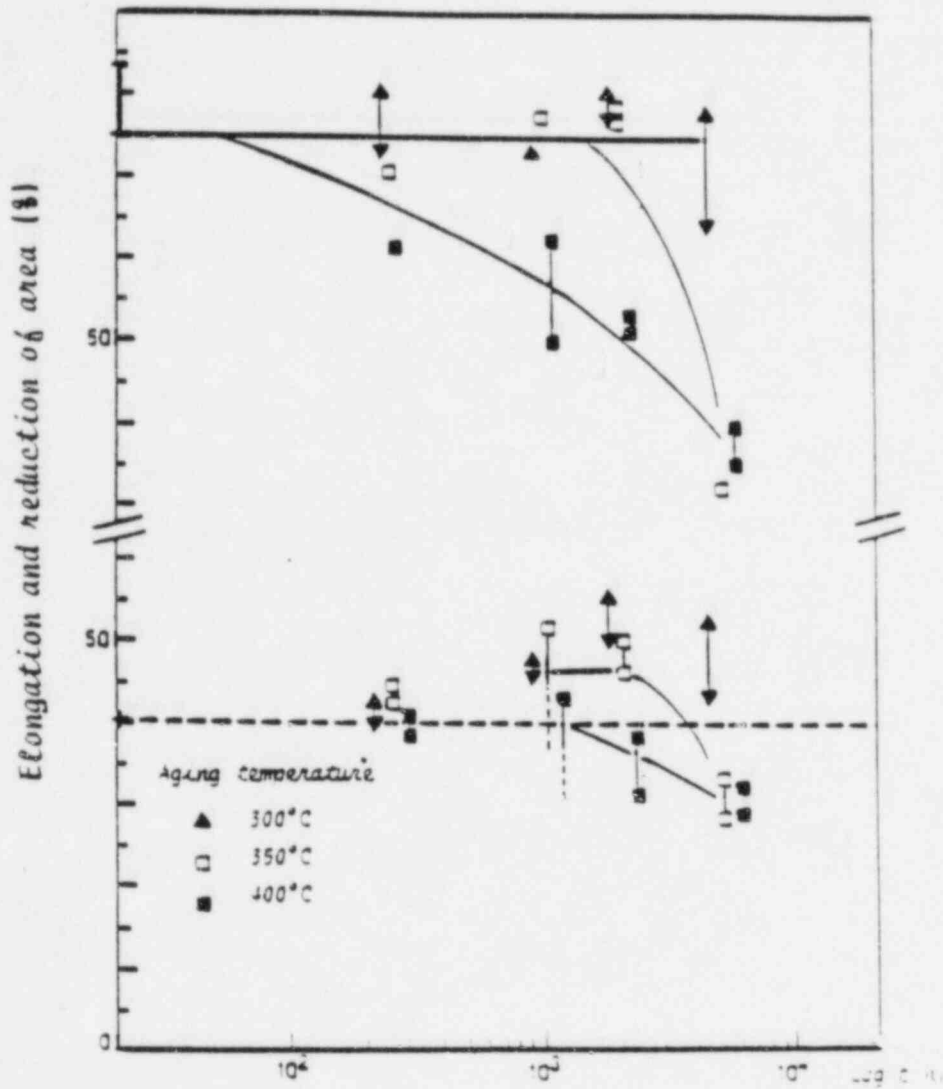


Figure 2.4-5: Heat B Elongation and reduction of area as a function of time of aging

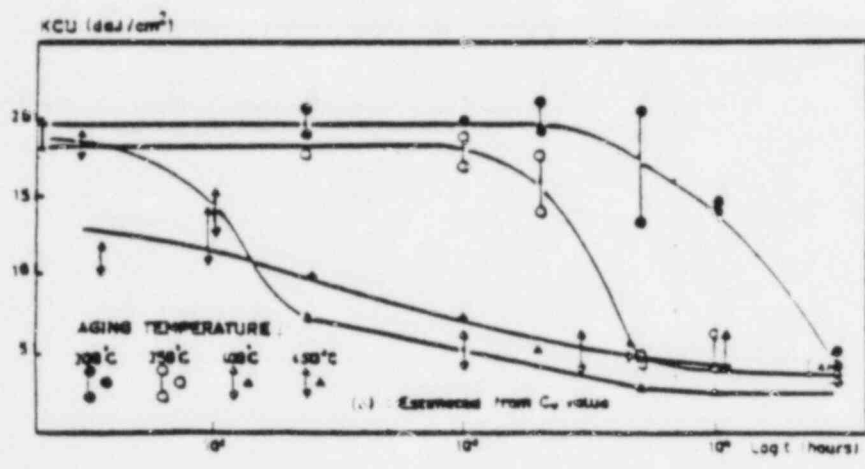


Figure 2.4-6: Heat B KCU impact toughness as a function of time.

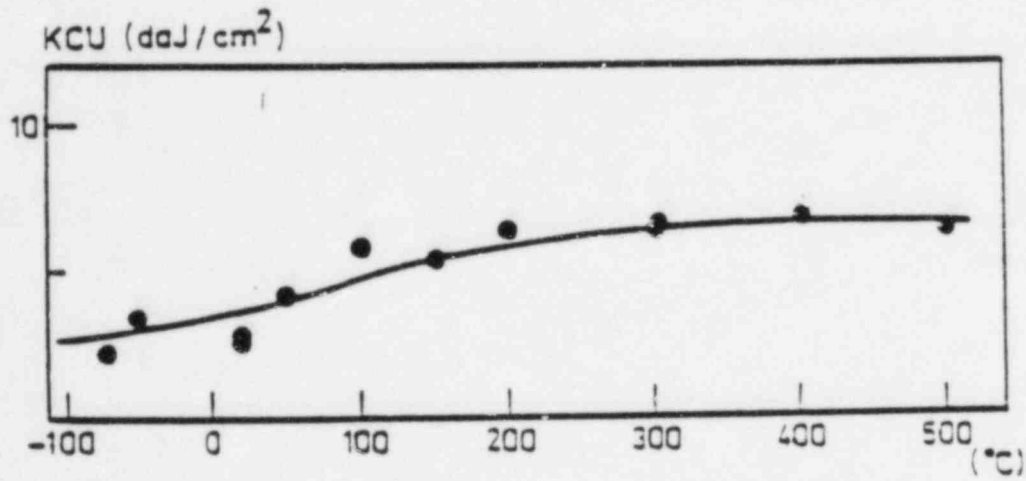


Figure 2.4-7: Heat B Influence of test temperature on KCU impact toughness after aging 10,000 hours at 400°C



Figure 2.4-8: J- $\Delta a$  Curves for welds B and D.  
Room temperature (interrupted tests)

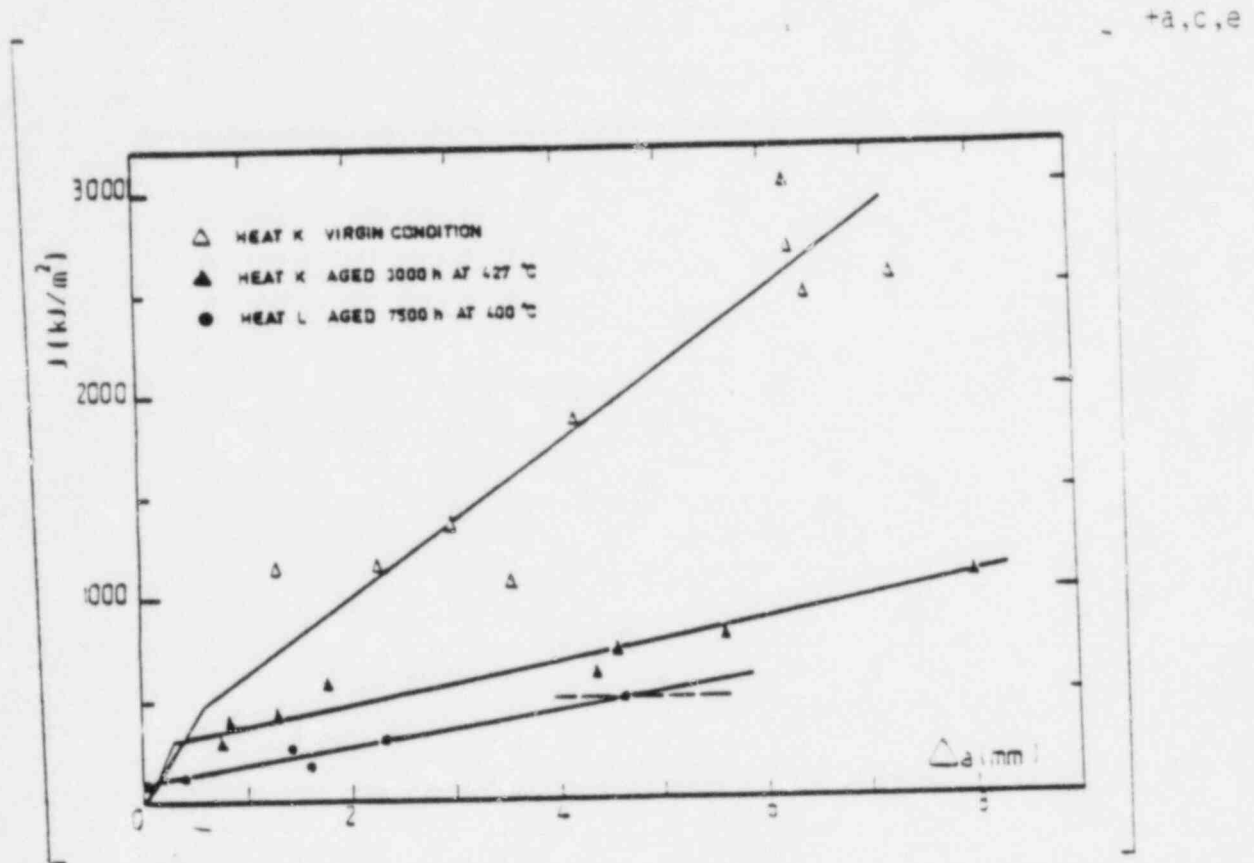


Figure 2.4-9: J- $\Delta a$  Curves for virgin and aged cast stainless steel



Figure 2.4-10: Heat L J- $\Delta a$  Curves at different temperatures  
Aged material (7500 hours at 400°C)

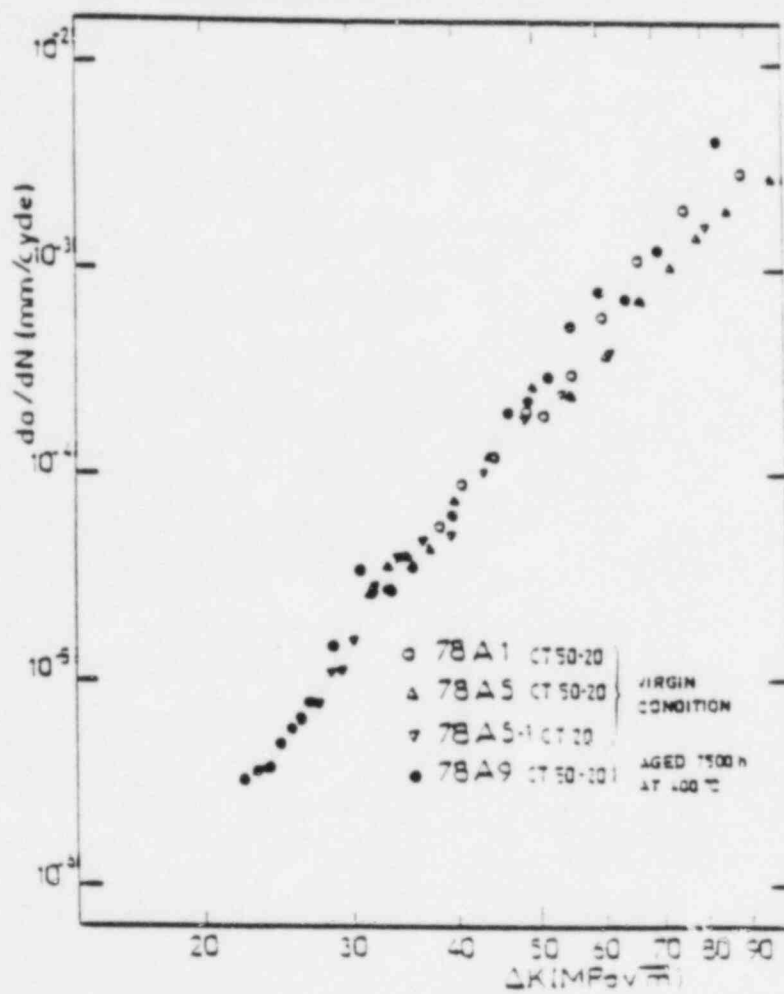


Figure 2.4-11: Heat L Fatigue crack growth rate at room temperature for virgin and aged material

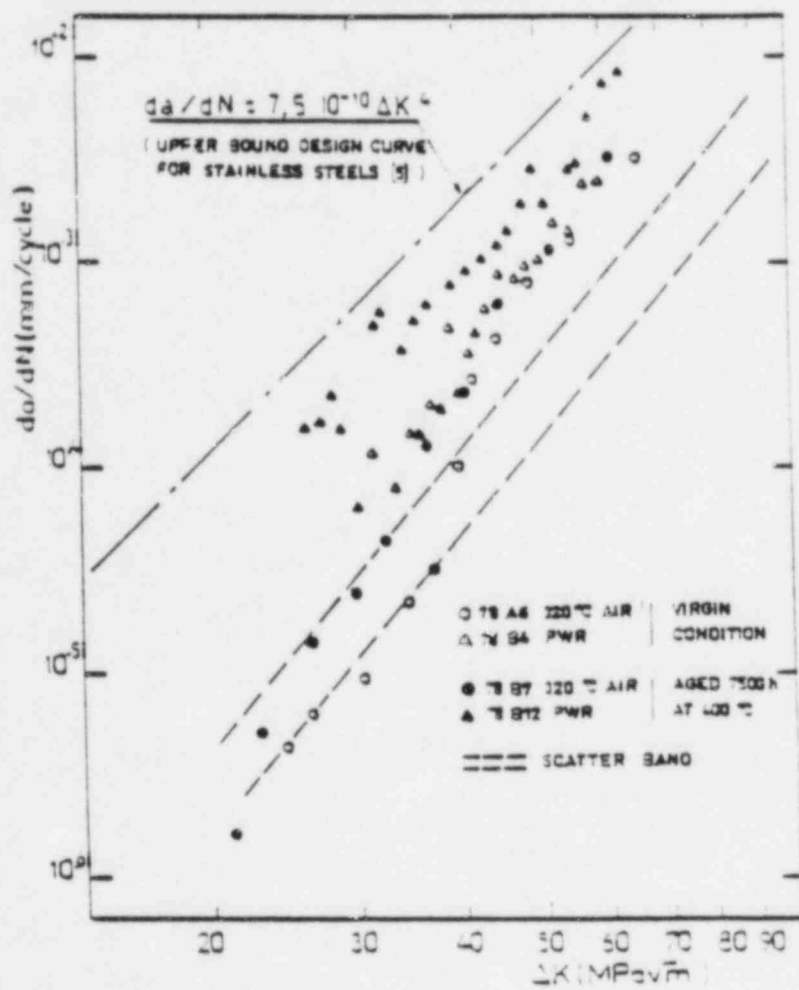


Figure 2.4-12 Heat L Fatigue crack growth rate at 320°C in air and in PWR environment (1 cm)

-+a,c,e

Figure 2.5-1 Charpy U-Notch Energy at Room Temperature  
for Heat L as a Function of Aging at 750°F  
(400°C)

ta,c,e



Figure 2.5-2 Charpy V-Notch Energy at Room Temperature and 550°F for Heat 1  
After Thermal Aging at 750°F for 7500 Hours

-a.c.

Figure 2.5-3 J-Integral Results of 200°F from Heat L

-a.c  
-

Figure 2.5-4 J Integral Results at 600°F from Heat L



FIGURE 2.5-5    FIGURE 25 OF SLAMA'S MONTEREY PAPER: HEAT L -  
J- $\Delta a$  CURVES AT DIFFERENT TEMPERATURES. AGED MATERIAL  
(7500 HOURS AT 400°C)

WESTINGHOUSE PROPRIETARY CLASS 3

SECTION 3

MECHANISMS OF THERMAL AGING

Page

WESTINGHOUSE PROPRIETARY CLASS 3

7-18-01

+a,c,e

WESTINGHOUSE PROPRIETARY CLASS 2

-3.0.8

Therefore, it may be concluded that the model of Slama, et. al [4] is consistent with the conclusions of independently conducted metallurgical studies of thermal aging behavior. The mechanism of aging is [the precipitation of a chromium-rich phase,] which occurs in the range of operating temperatures for pressurized water reactors [(288-316°C),] and also occurs at temperatures exceeding 400°C, so the data from accelerated aging studies can be used to predict the behavior at operating temperatures.



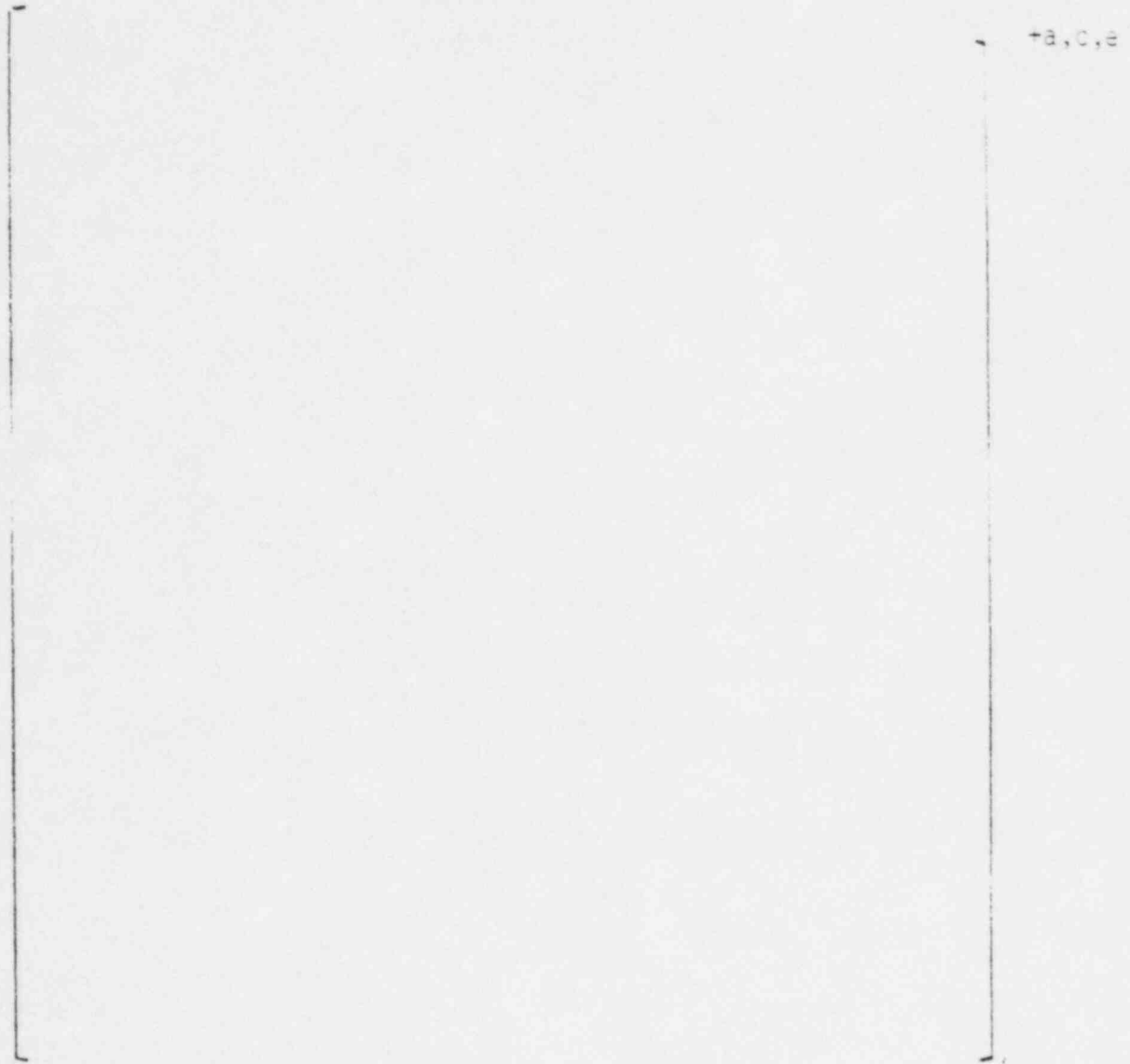


Figure 3-1 Low Temperature miscibility gap in Fe-O<sub>2</sub> system

1-a, c, e



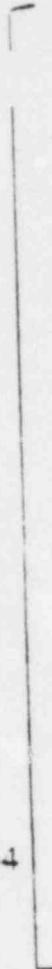


Figure 3-4

TEMPERATURE (°C)



Figure 3-5



Figure 3-6

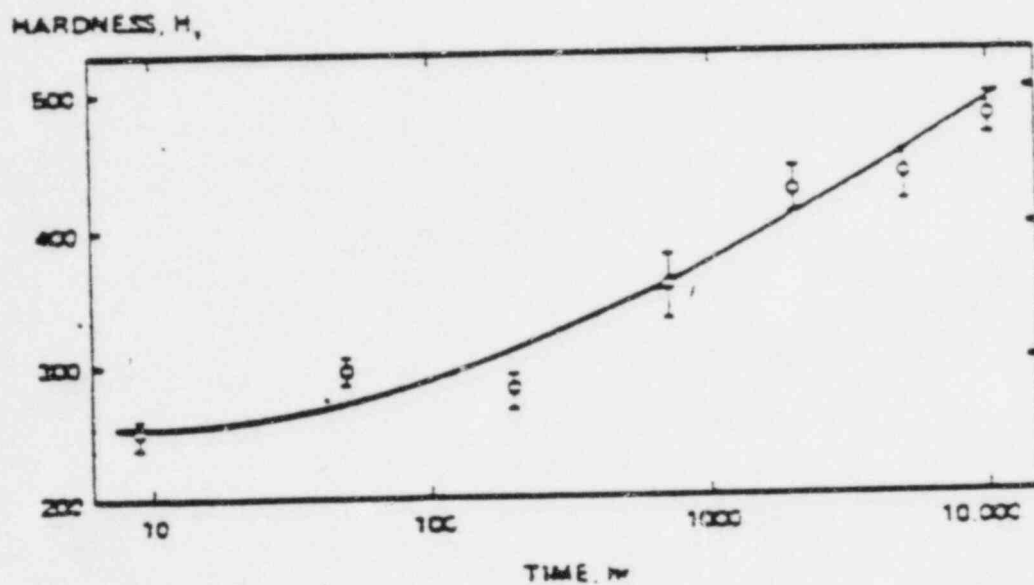


Figure 3-7 Increase in hardness of Fe-32 at 0.3 Cr during aging at 470°C [16]

SECTION 4

FRACTURE ASSESSMENT IN AUSTENITIC STAINLESS STEEL PIPING

4.1 METHODOLOGY

Determination of the conditions which can lead to failure in stainless steel must be done with plastic fracture methodology because of the large amount of deformation accompanying fracture. The state-of-the-art in plastic fracture prediction is such that several viable methods are available, including:

- o Tearing instability
- o R-6 failure assessment method
- o Direct application of J-R curves

All of these methods include some method of dealing with the stable crack growth which precedes final failure in ductile materials. This sub-critical extension of the crack is accomplished by an increasing toughness of the material, as displayed graphically in the J-integral R curves discussed in the previous section.

#### 4.2 EXPERIMENTAL VERIFICATION

Several experiments were completed at Battelle Memorial Institute to consider this type of loading, and a prediction method similar in form to the above equation was used. The above method accurately accounts for the piping internal pressure as well as imposed axial force as they affect the limit moment. [

+a,c,e

]†

The prediction equation for uniform circumferential flaw at the inside diameter is a simplification of the above equation where the flaw length  $a$  is set at zero, and the thickness is adjusted for the presence of the flaw.

The equivalent prediction for a through-wall longitudinally oriented flaw was suggested by Eiber et al. [23], and shown to be applicable to a number of piping geometries and materials in a sizeable number of tests. Axially flawed pipes are largely unaffected by imposed bending moments, and the limit pressure is given by:

$$P_{LIM} = \sigma_L t / R_m$$

where

$$\sigma_L = [1.28 - 1.4\lambda + 0.809\lambda^2 - 0.219\lambda^3 + 0.0217\lambda^4] \sigma_f$$

(curve-fit Ref. [24])

$$\lambda = a / \sqrt{Rmt}$$

$$a = \text{crack length}$$



WESTINGHOUSE PROPRIETARY CLASS 3

WESTINGHOUSE PROPRIETARY CLASS 3

#### 4.4 STABILITY ANALYSIS BASED ON TEARING MODULUS

In addition to the plastic instability methodology detailed earlier in this section, the stability of flaws postulated in the reactor coolant piping can also be evaluated by characterization of the local crack tip behavior. The behavior of the pipe in the crack tip region was studied through the various stages which can lead to failure, that is crack tip blunting, initiation, extension and then crack instability. Material characterization is in terms of the J-integral R curve, and the evaluation of integrity can be accomplished in two stages. The first stage is the evaluation of whether a postulated flaw will initiate under the applied loading, based on comparison with  $J_{IC}$  properties of the material. The second stage is the evaluation of stability based on applied and material values of the tearing modulus. The theoretical background and experimental validation of the tearing modulus approach to stability of cracked pipes were provided in Reference 26.

be 6174 in-lb/in<sup>2</sup>, which exceeds the value of  $J_{IC}$  for the cast piping at end of life conditions. Therefore crack initiation cannot be avoided under this worst case loading, and the stability of the crack must be evaluated.

The value of applied  $T$  was calculated based on the J-integral calculations in Reference 27, according to the following upper bound equation proposed by Tada [26]:

$$T_{app} = F_1 \frac{L}{R_m} + F_2 \frac{JE}{\sigma_f^2 R_m}$$

where:

- $L$  = length of reactor coolant hot leg pipe
- $R_m$  = mean radius of hot leg pipe
- $\theta$  = half the angle subtended by the through-wall crack at the center of pipe cross section, (Figure A-1)
- $T$  = hot leg wall thickness
- $\sigma_f$  = flow stress
- $E$  = modulus of elasticity
- $\alpha$  = angular location of neutral axis, (same as  $\beta$  in Figure A-1)
- $F$  = the axial load on the pipe

$$F_1 = \frac{2}{\pi} (\sin \alpha + \cos \theta)^2$$

$$F_2 = \frac{1}{2} \frac{(\cos \alpha - 2 \sin \theta)}{(\sin \alpha + \cos \theta)}$$

$$\alpha = \frac{1}{2} \theta + \frac{\pi}{2} \left[ \frac{F}{\sigma_f (2\pi R t)} \right]$$

-a,c,e

IMAGE EVALUATION  
TEST TARGET (MT-3)

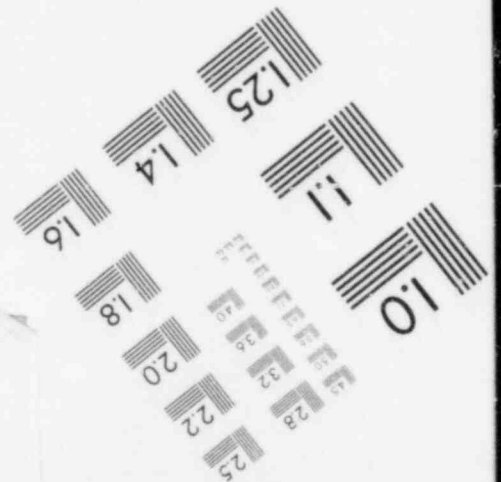
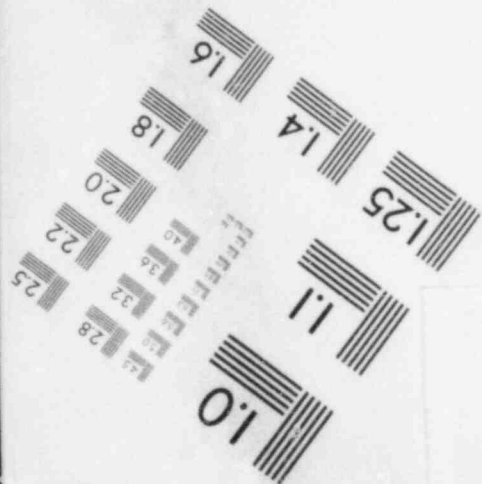
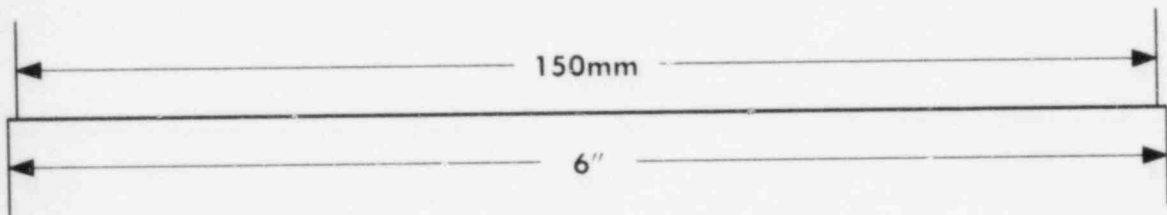
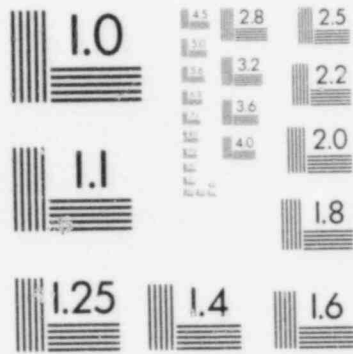
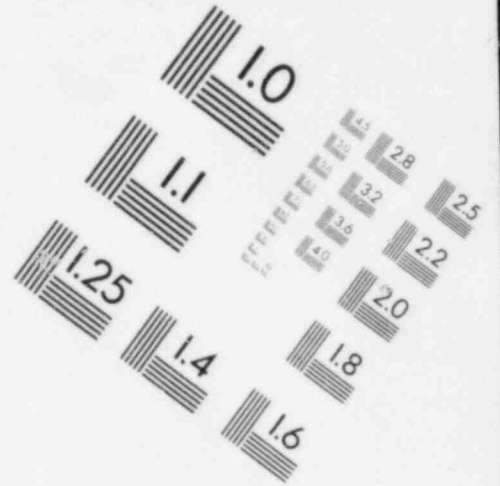
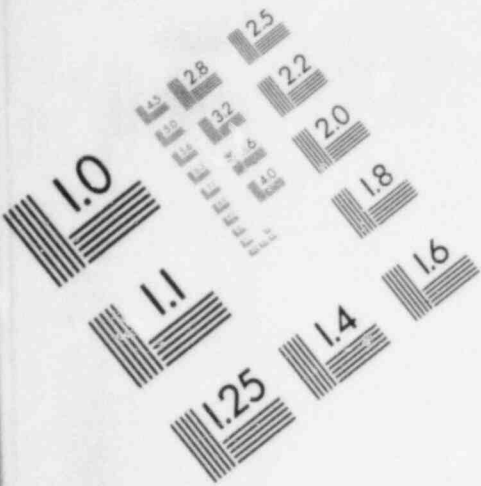
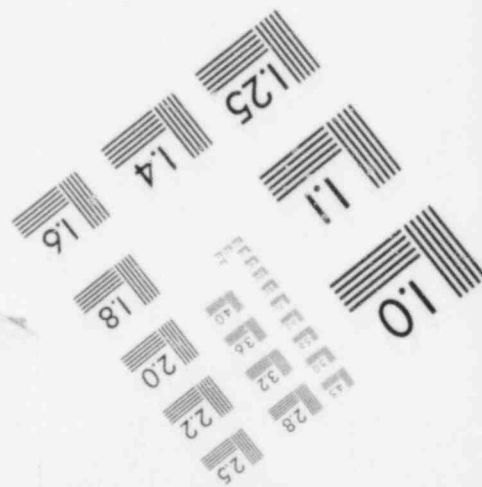
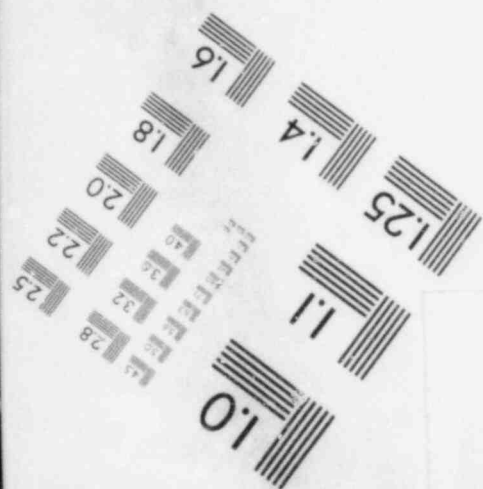
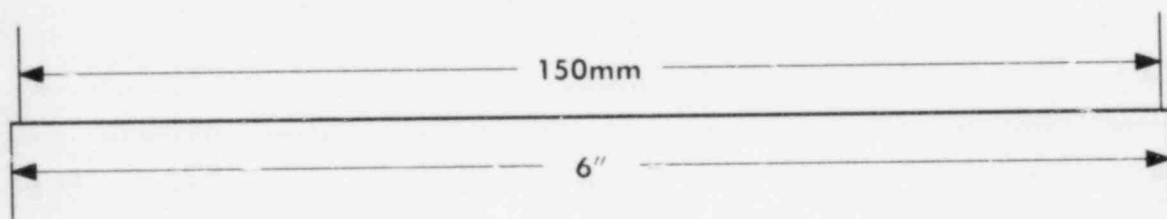
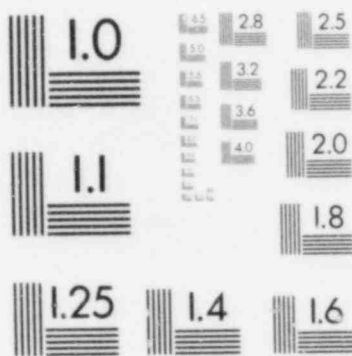
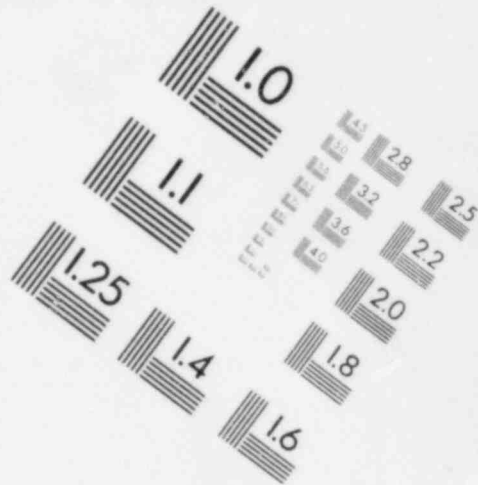
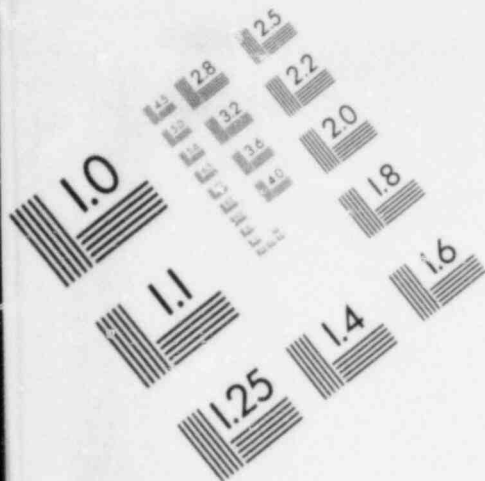
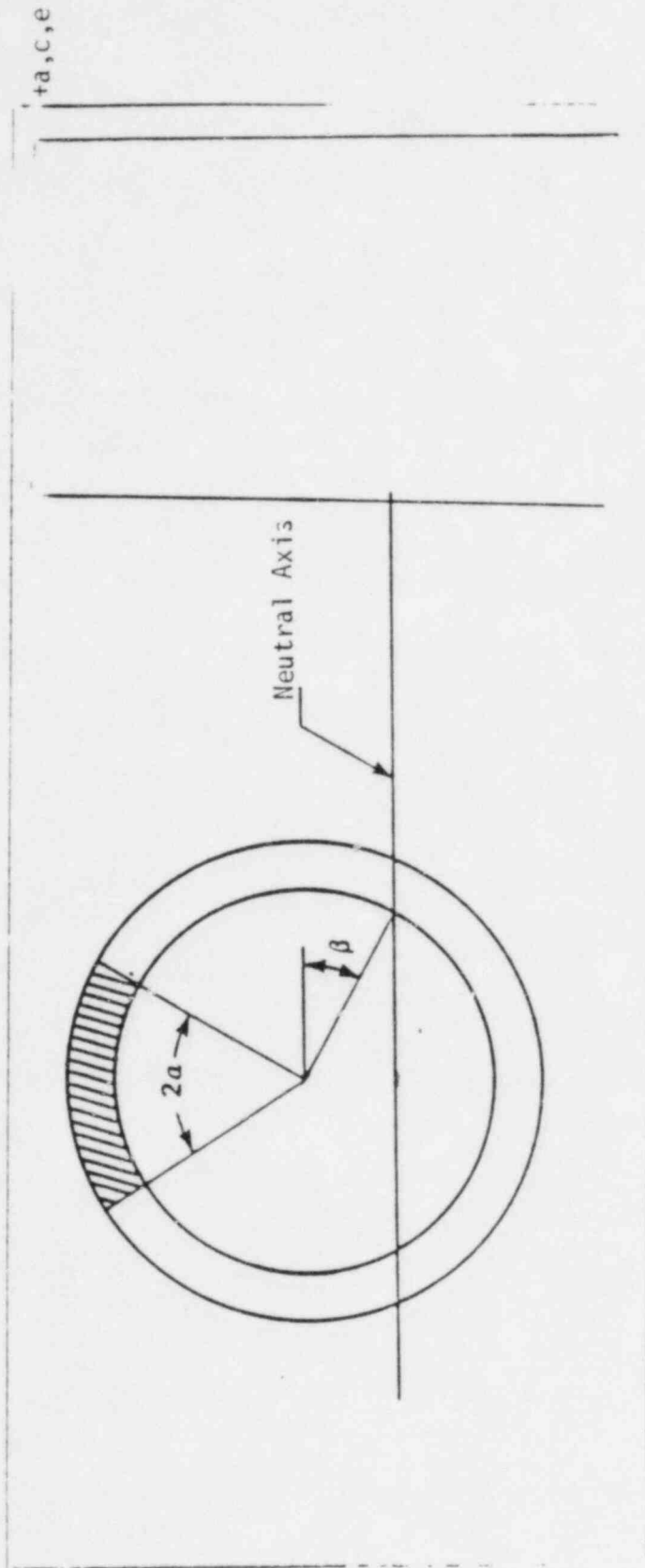


IMAGE EVALUATION  
TEST TARGET (MT-3)



WESTINGHOUSE PROPRIETARY CLASS 3

— 73



$\tau_{a,c,e}$   
] Stress Distribution

Figure 4-1 I

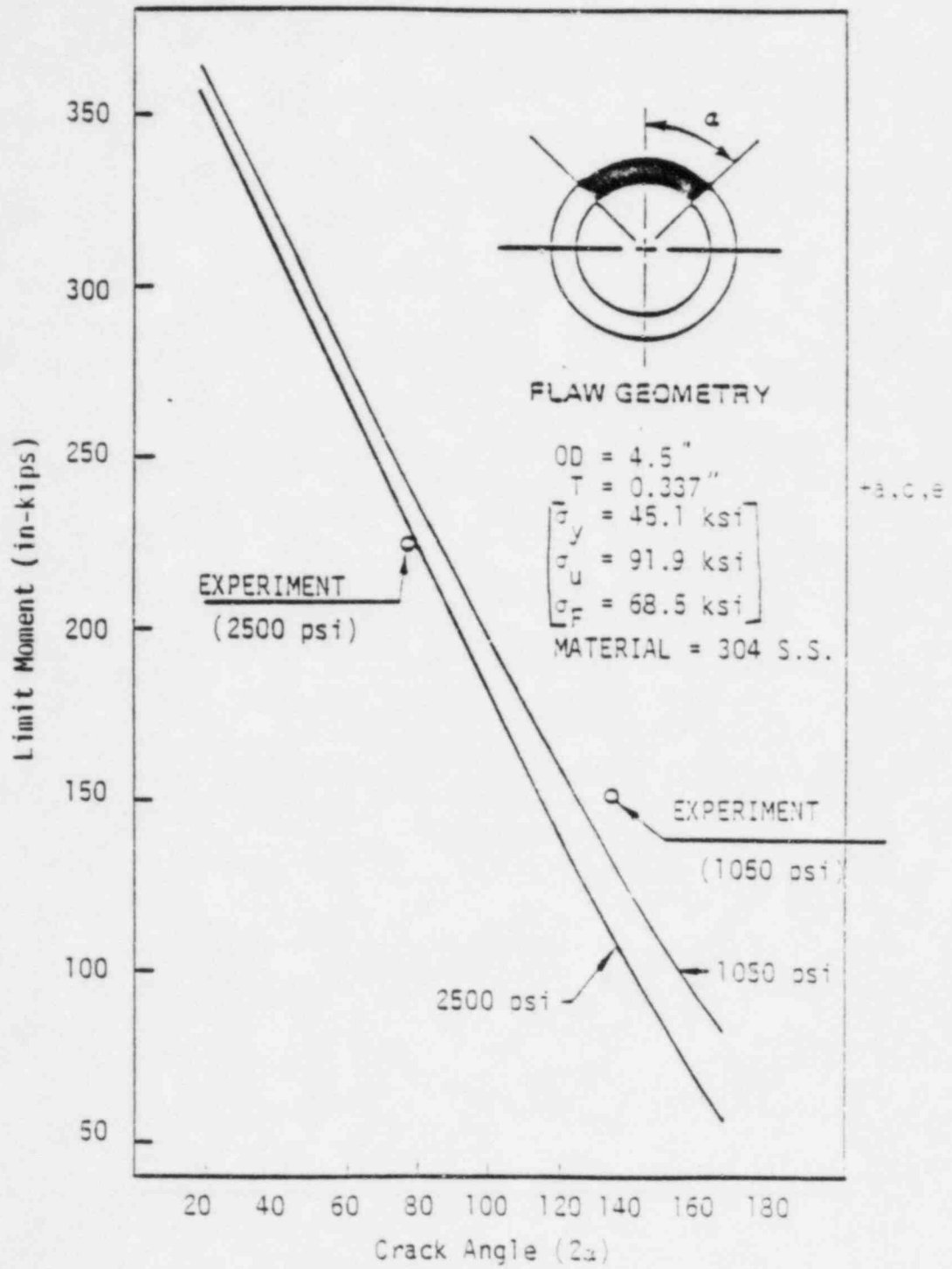


Figure 4-2 Comparison of [ ] predictions with Experimental Results

+a,c,e

$\sigma/\bar{\sigma}$

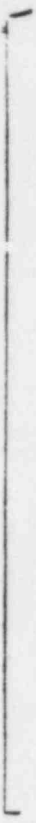


Figure 4-3 Comparison of Failure Predictions with Experimental Results of [24]

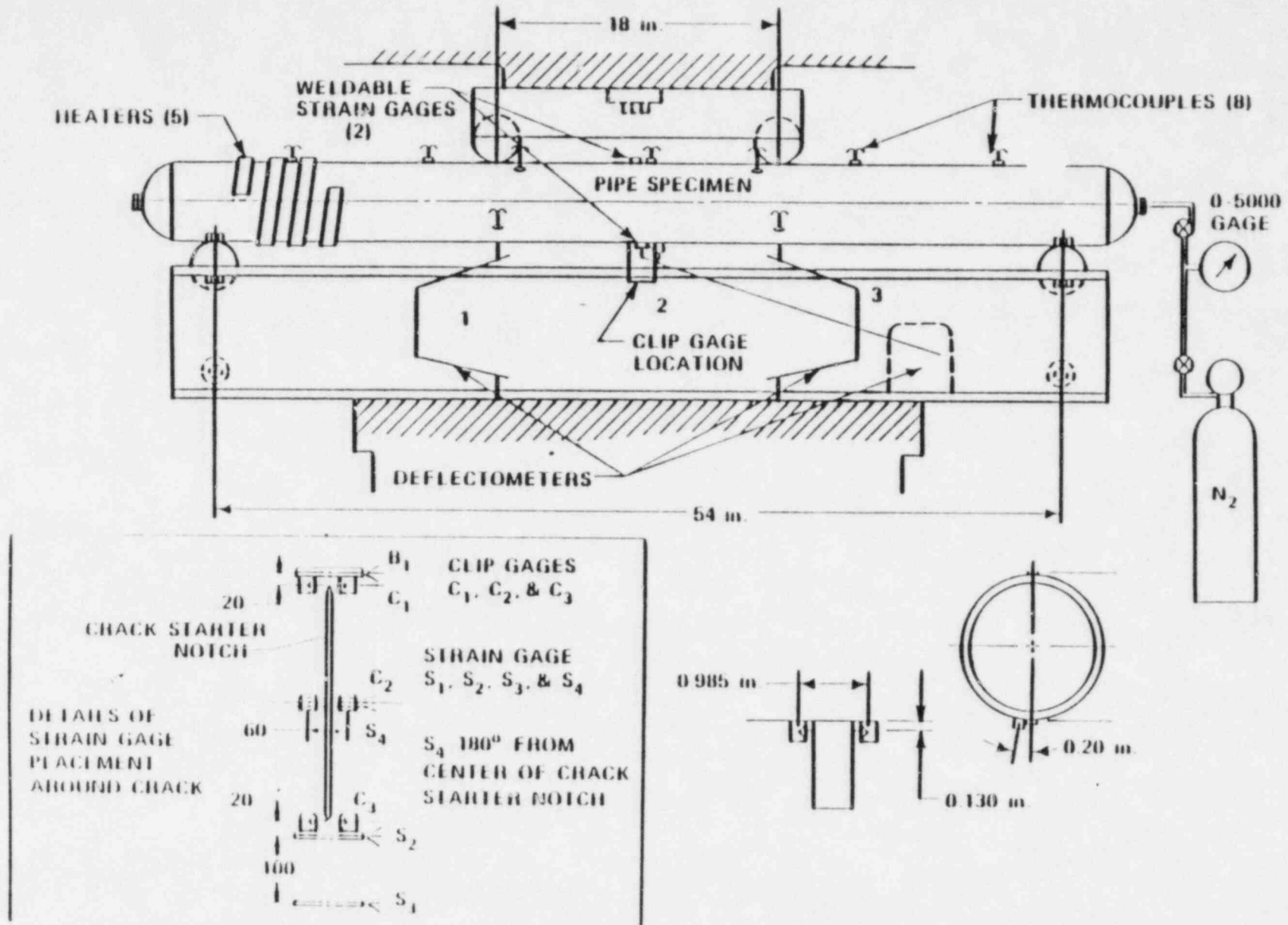
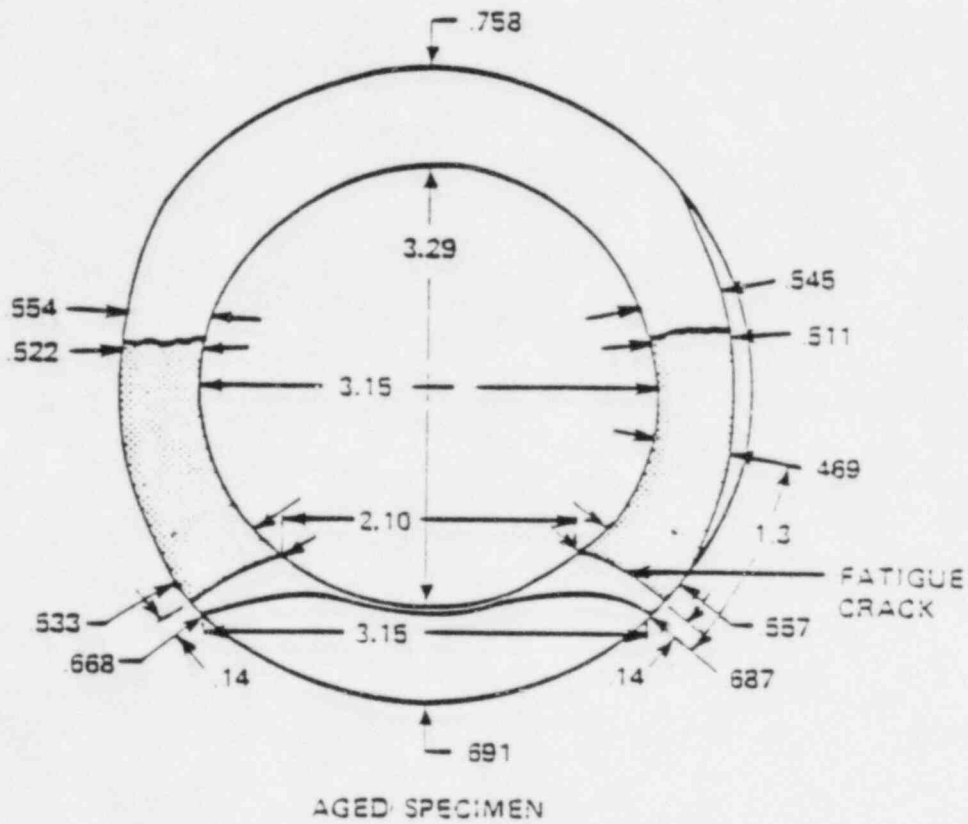
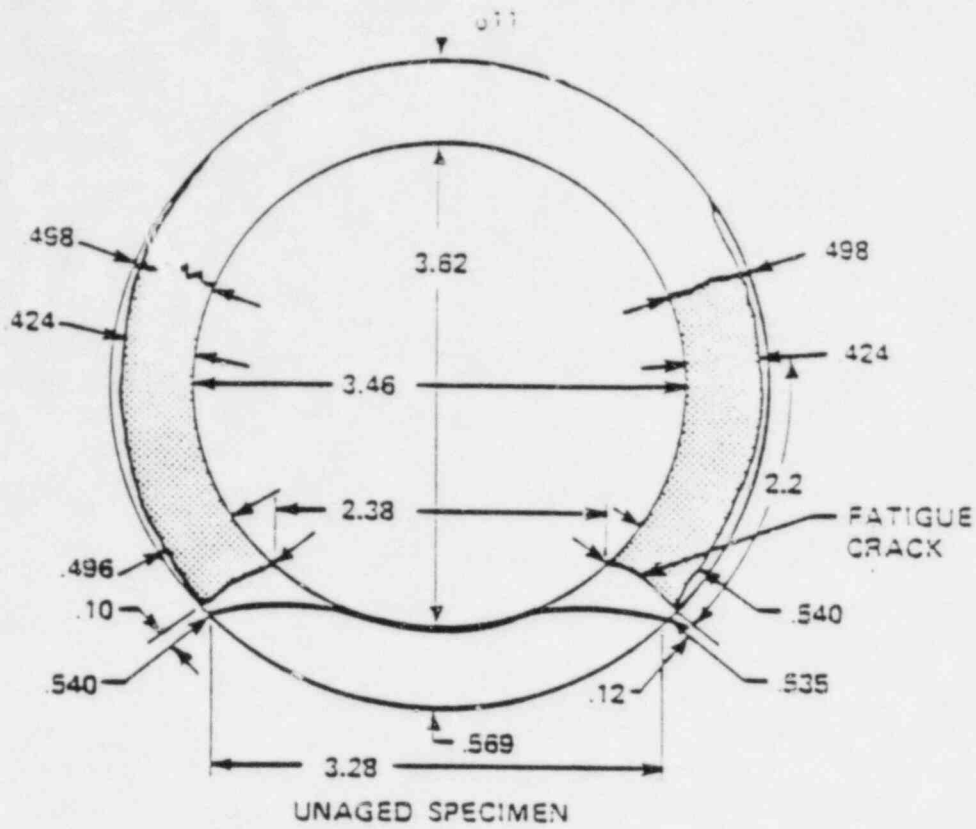


Figure 4-4 Test Assembly of Four Fe-50Ni



(TO CONVERT DIMENSIONS SHOWN HERE IN INCHES TO DIMENSIONS IN cm, MULTIPLY BY 2.54.)

Figure 4-5 Pertinent Dimensions of Aged and Unaged Pipes after Testing

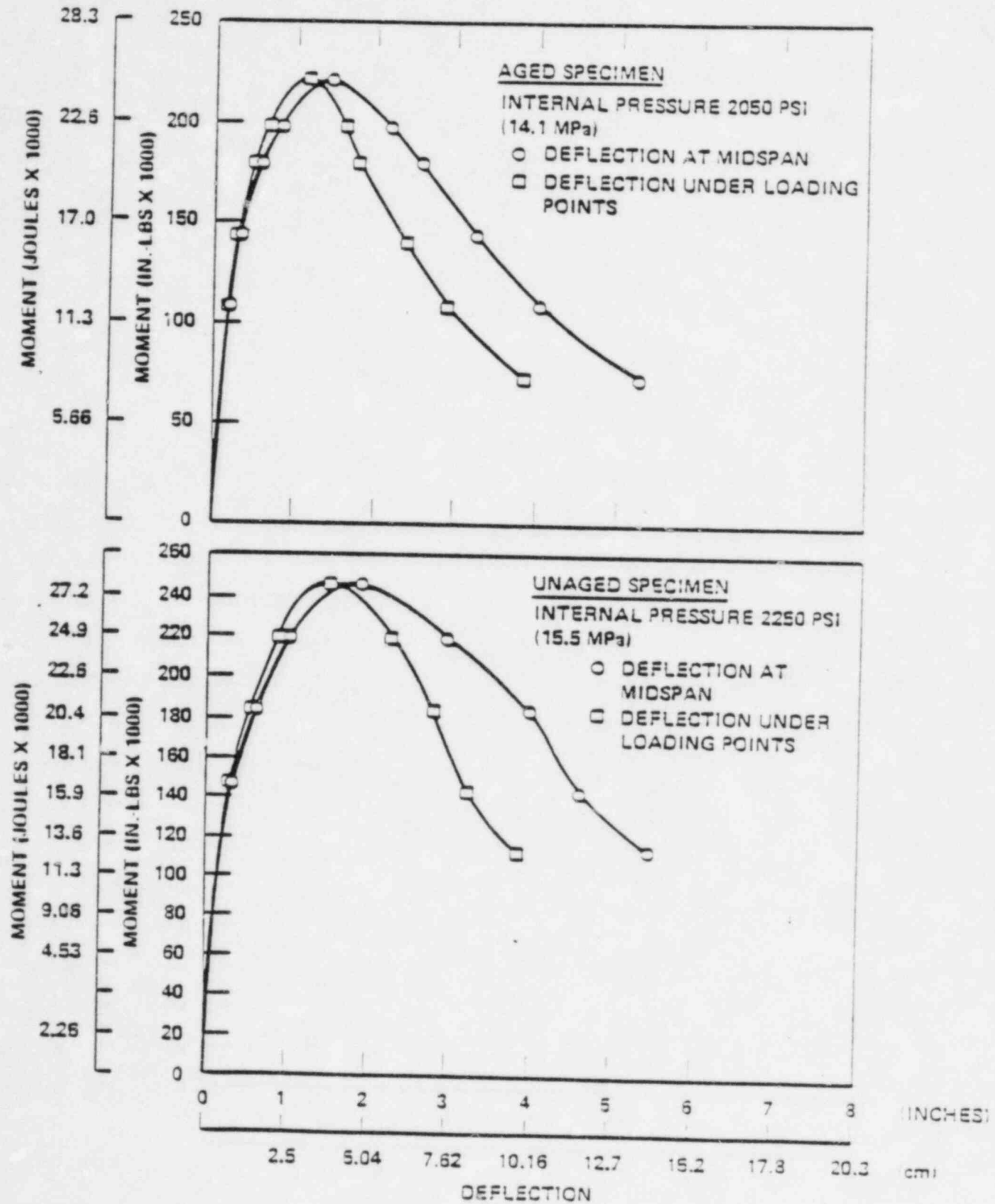


Figure 4-6 Moment-Deflection Curves for Aged and Unaged Four Inch 30 Pipes



Figure 4-7 Comparison of Predicted and Actual Limit Moment for Tests of Aged and Unaged Pipes

SECTION 5

EFFECTS OF THERMAL AGING ON  
WESTINGHOUSE SUPPLIED CENTRIFUGALLY CAST  
REACTOR COOLANT PIPING

5.1 PRODUCTION AND QUALITY ASSURANCE

Stainless steel reactor coolant piping used in nuclear steam supply systems must be produced and inspected to ensure certain standards of quality and reliability. [

]

Once the pipe is cast, it is inspected and tested thoroughly prior to being put into service. [

]

[of pipe at room temperature, while a single high temperature tensile test is done on each heat at 650°F. Several nondestructive testing procedures as well are performed on the finished pipe. Radiography of 100 percent of each pipe's wall volume is done according to ASME Section III, Paragraph NB-2573. Liquid penetrant examination is conducted on all surfaces of the pipe in accordance with the ASME Code and G-678864. The latter lists several more stringent requirements than the Code for surfaces less than several inches from the ends of each pipe. In addition, the ASME Code requires a visual inspection for defects such as tears, cracks, and scale, while G-678864 sets maximum roughness standards for the pipe surfaces.] All of these safety-related requirements provide for quality assurance in the finished product.

## 5.2 END-OF-LIFE TOUGHNESS PREDICTIONS

The thermal aging of austeno-ferritic stainless steel occurs at reactor coolant loop temperatures as a chromium rich phase, alpha prime ( $\alpha'$ ), precipitates in the ferritic phase. The precipitation of the  $\alpha'$  stage is responsible for the hardening and embrittlement experienced by the steel.

- for 10,000 hours aging at 400°C:  

$$\text{KCU (daJ/cm}^2\text{)} = 52.5 - 2.19 (\text{ Si} + \text{ Cr} + \text{ Mo}) + 46/\delta \quad (\text{Eq. 5-1})$$
- for 30,000 hours aging at 400°C:  

$$\text{KCU (daJ/cm}^2\text{)} = 32.8 - 1.39 (\text{ Si} + \text{ Cr} + \text{ Mo}) + 60/\delta \quad (\text{Eq. 5-2})$$

where  $\delta$  = ferrite, as measured by the Schoefer diagram.

The first of these equations (5-1) was determined by Slama et. al. [4] to result in Charpy values equivalent to the minimum Charpy values expected during service for CF8M cast stainless steel. Equation 5-2 was shown to be applicable to CF8 and CF8A materials. These equations are applicable regardless of the temperature of operation of the piping (which will of course be different in the hot and cold legs). Slama et. al. calculated using time-temperature equivalencies that the aging times at 400°C corresponding to the total 32 year service life for CF8M ranged from 13,000 hours for the cold leg (290°C) to 34,000 hours for the hot leg (320°C). In studying the available data, however, they found that the minimum properties were obtained only after 10,000 hours and therefore this time was used. Lifewise, for CF8 (and CF8A) the equivalent aging times at 400°C were calculated to be 30,000 hours for the cold leg and 60,000 hours for the hot leg. Again they found that the minimum properties were obtained only after 30,000 hours for CF8, so that time was used in the model, to predict the maximum effects of service.

The models given in equations 5-1 and 5-2 were found to be very good fits of the available Fischer data, and were tested on the data obtained by Slama, et al., [4]. The correlation coefficients for the fits were 0.967 for equation 5-1 and 0.987 for equation 5-2. The standard deviations were 0.95 daJ/cm<sup>2</sup> and 0.57 daJ/cm<sup>2</sup>, respectively. The equations were based on the actual ferrite percentages determined by Fischer on 15 heats of cast stainless steel, using magnetic measurement. Slama's verification of the model was accomplished using the Schoefer diagram values of ferrite content, as normally reported on material test certificates. The ferrite levels determined in this manner were found to be within 1-3 percent of levels determined magnetically and by quantitative metallography, and the model predicted the behavior of Slama's additional heats very well. The data base used to develop the model included ferrite contents ranging from 6-42 percent.

WESTINGHOUSE PROPRIETARY CLASS 3

5.3 PLANT SPECIFIC END-OF-LIFE REACTOR COOLANT PIPING TOUGHNESS

a, c, e

TABLE 5-1

CHEMICAL AND PHYSICAL PROPERTIES OF PLANT A REACTOR COOLANT PIPING

c,e

---

TABLE 5-2

---

1a, C, t

TABLE 5-3

CHEMICAL AND PHYSICAL PROPERTIES OF PLANT C REACTOR COOLANT PIPING

†a, C, t

TABLE 5-4

CHEMICAL AND PHYSICAL PROPERTIES OF PLANT D REACTOR COOLANT PIPING

[Empty table area]

†a, c,

CHEMICAL AND PHYSICAL PROPERTIES OF PLANT E REACTOR COOLANT PIPING

TABLE 5-b

ta, c, e

TABLE 5-6

CHEMICAL AND PHYSICAL PROPERTIES OF PLANT F REACTOR COOLANT PIPING

ta, c, e

TABLE 5-7

CHEMICAL AND PHYSICAL PROPERTIES OF PLANT G REACTOR COOLANT PIPING



TABLE 5-9

CHEMICAL AND PHYSICAL PROPERTIES OF PLANT 1 REACTOR COOLANT PIPING

ta, c, e

WESTINGHOUSE PROPRIETARY CLASS 3

\_\_\_\_\_

\_\_\_\_\_

ta, c, e

TABLE 5-10

CHEMICAL AND PHYSICAL PROPERTIES OF PLANT J REACTOR COOLANT PIPING

WESTINGHOUSE PROPRIETARY CLASS 3

SECTION 6

SUMMARY AND CONCLUSIONS

WESTINGHOUSE PROPRIETARY CLASS 3

## SECTION 7

## REFERENCES

1. F. H. Beck, E. A. Schoefer, J. W. Flowers, M. E. Fontana, "New Cast High Strength Alloy Grades by Structural Control", ASTM STP 369 (1965) - p. 159.
2. E. I. Landerman and W. H. Bamford, Fracture Toughness and Fatigue Characteristics of Centrifugally Cast Type 316 Stainless Steel After Simulated Thermal Service Conditions, presented at the Winter annual Meeting of the ASME, San Francisco, CA. December 10-15, 1978 (MPC-8, ASME).
3. W. H. Bamford, E. I. Landerman and E. Diaz, Thermal Aging of Cast Stainless Steel and Its Impact on Piping Integrity. Presented at ASME Pressure Vessels and piping Conference, Portland, Oregon June 1983. To be published in ASME Trans.
4. G. Slama, P. Petrequin, S. H. Masson and T. R. Mager, Effect of Aging on Mechanical Properties of Austenitic Stainless Steel Casting and Welds, presented at SMIRT 7 Post Conference Seminar 6 - Assuring Structural Integrity of Steel Reactor Pressure Boundary Components, August 29/30, 1983, Monterey, Ca.
5. Standard Test Method for  $J_{IC}$ , A measure of Fracture Toughness. 1983 Annual Book of Standards, Section 3 Volume 03.01, American Society for Testing and Materials, 1983, pp. 762-780.
6. W. H. Bamford and A. J. Bush, "Fracture Behavior of Stainless Steel," Elastic-Plastic Fracture, STP 668, American Society for Testing and Materials, 1978.
7. W. H. Bamford, "Fatigue Crack Growth of Stainless Steel Piping in a Pressurized Water Reactor Environment", ASME Paper 77-PVP-34, Sept. 77.

WESTINGHOUSE PROPRIETARY CLASS 3

8. K. Walker, "The Effect of Stress of Stress Ratio During Crack Propagation and Fatigue for 2024-T3 and 7075-T6 Aluminum," Effects of Environment and Complex Load History on Fatigue Life, ASTM-STP-462. American Society for Testing and Materials, 1970, pp. 1-14.
9. Fisher, Dulis, and Carroll, Trans. ASME, Vol. 197, pp. 690, 1983.
10. R. N. Wright, "Toughness of Ferritic Stainless Steels," ASTM STP 706, R. A. Lula Ed., ASTM 1980 p. 2-33.
11. R. O. Williams and H. W. Paxton, Trans. ASME, 185, 358 (1957).
12. M. V. Rao and W. A. Tiller, Scripta Met., 6 (1972).
13. Y. Imai, M. Izumiyama and T. Masumoto, Sci. Rep. Res. Inst. Tonoku University, SER A, 18, 56 (1966).
14. D. Chandra and L. H. Schwartz, Met. Trans. 2, 511 (1971).
15. T. Nishizawa, M. Hasebi and M. Ko, Acta Met. 27, 817 (1976).
16. S. S. Brenner, M. K. Miller and W. A. Soffa, Scripta Met. 16, 831 (1982).
17. T. J. Nichol, Met. Trans. 8A, 229 (1977).
18. I. A. Franson, Met. Trans. 5, 2257 (1974).
19. R. Stickler and A. Vinckier, Trans. ASME, 54: 362 (1961).
20. B. Weiss and R. Stickler, Met. Trans., 3: 951 (1972).
21. J. C. Gerdeen, "A Critical Evaluation of Plastic Behavior Data and a Unified Definition of Plastic Loads for Pressure Components," in Welding Research Council Bulletin 254, November 1979.

22. M. F. Kanninen, D. Broek, C. W. Marschall, E. F. Rybicki, S. G. Sampath, F. A. Simonen, and G. M. Wilkowski, "Mechanical Fracture Predictions for Sensitized Stainless Steel Piping with Circumferential Cracks", EPRI-NP-192, September, 1976.
23. R. J. Eiber, W. A. Maxey, A. R. Duffy, and T. J. Atterbruy, "Investigation of the Initiation and Extent of Ductile Pipe Rupture", BMI 1866, July 1969.
24. H. Zeibig, and F. Fortmann, "Fracture Behavior of Ferritic and Austenitic Steel Pipes," Proceedings Second Conference on Structural Mechanics in Reactor Technology," Berlin 1973, F4/8.
25. "Instability Predictions for Circumferentially Cracked Pipe", M. F. Kanninen, et. al., Electric Power Research Institute Project T118-2 Final Report, 1981.
26. Paris, P. and Tada, H. "The Application of Fracture Proof Design Methods Using Tearing Instability Theory to Nuclear Piping Postulating Circumferential Through-wall Cracks," NUREG/CR 3464, US NRC, 1983.
27. S. S. Palusamy and A. J. Hartman, "Mechanistic Fracture Evaluation of Reactor Coolant Pipe Containing a Postulated Through-Wall Crack", Westinghouse Electric Corp. WCAP-9558 Rev. 2, May 1982 (Proprietary Class 2).
28. A. Trautwein, and W. Gysel, "Influence of Long-Time Aging of CF8 and CF8M Cast Steel at Temperatures Between 300 and 500 Degree C on the Impact Toughness and the Structural Properties. ASTM STP-756, p. 165, (1981).
29. ASTM Standard A800-82, "Estimating Ferrite Content in Austenitic Alloy Castings". Section 1, Volume 01.01, American Society for Testing and Materials, 1983, p. 543.